TÉCNICO LISBOA

Polycaprolactone nanoparticles as carriers for delivery of enzymes into cells

Mariana Machado Correia da Cunha

Thesis to obtain the Master Degree in

Bioengineering and Nanosystems

Supervisors:
Professor Prasad Shastri
Professor Maria Ângela Cabral Garcia Taipa Meneses de Oliveira

Examination Committee

Chairperson: Professor Gabriel António Amaro Monteiro
Supervisor: Professor Maria Ângela Cabral Garcia Taipa Meneses de Oliveira
Member of the Committee: Professor Duarte Miguel de França Teixeira dos Prazeres

June 2020

Preface

The work presented in this thesis was performed at the Institute fur Makromolekular Chemie (ShastriLab), in the Albert-Ludwigs Freiburg University, between October and March, 2019-2020. The thesis was supervised by Professor Doctor Prasad Shastri and MSc. Cristopher Dresler and co-supervised at Instituto Superior Técnico by Professor Doctor Maria Ângela Cabral Garcia Taipa Meneses de Oliveira.

I declare that this document is an original work of my own authorship and that it fulfills all the requirements of the Code of Conduct and Good Practices of the Universidade de Lisboa.

ACKNOWLEDGEMENTS

During these six months, this project developed and became one of the most important things that I did in my life. It was a challenger and tricky project, that helped my growth as a person, scientist, and professional. I had the opportunity to start a research project from the ground, which implies hard work. Doing and re-doing assays a couple of times until we get it right, and in the end, we obtain knowledge, tools, and resilience that are extremely important for our professional and personal lives.

Also, I want to say thank you to Professor Doctor Prasad Shastri for having given me this opportunity to come to the Institute fur Makromolekular Chemie. I learnt during these months and had contact with the incredible ShastriLab, that knows how to work, teach and is always open to help. And thank you for giving this opportunity to build, create something from zero, it was a fantastic journey. Through this adventure, I need to thank a person who was essential for the implementation of this project to Cristopher Dresler. He was a great teacher. I learned so much from him. He was always open to listening, helping, teaching, and thank for all the talks during the flow cytometry measurements. Thank you for supporting my growth as a person and a scientist. And thank you for all your patience with my mistakes.

In the ShastriLab, I also want to say thank to Merve Kuzuku and Grace Vera for becoming a part of this journey, to be incredible friends, and for helping me grow through knowledge share, and for all the dedikodo times. Also, I want to say thank you to all the bio lab team (especially Laurent Starck, Aijun Li, and Pan Wei) to help me all the times that I needed, for talks during quick breaks and all the jokes and laughs.

There is a person that I would like to say a special thank you, which is my supervisor from IST, Professor Doctor Maria Ângela Taipa, for all the guidance and journey that we built through this last year. Professor Ângela was always available and present through these times, was essential for my personal and professional growth, and supported me a lot during this adventure. I want to say thank you to Nova University and Instituto Superior Técnico for being my support, the places that I first contacted with science and in the best way possible, due to the incredible teachers that I had, colleagues, and friends. Mainly, I need to thank my bachelor thesis supervisors:

Professor Doctor Maria Alexandra Fernandes and Professor Doctor Pedro Viana Baptista, due to them I had my first contact with nanotechnology area, to a research project and they became an essential part of my professional growth, no matter how much time it passes.

Finally, I want to thank my family, especially my parents and my brother, for giving me the support that I needed not only through these months but for all of my life. My education, the places where I graduated, home, they were and are fundamental for my growth and to become a person that I want to be for always giving me a place where I feel safe.

RESUMO

A presente dissertação teve como principal objetivo o desenvolvimento de nanopartículas poliméricas como veículos de transporte de enzimas para células. As nanopartículas foram preparadas por nanoprecipitação de policaprolactona (PCL) modificada com óxido de propargil 3-metilpentanoato. A superóxido dismutase e a fosfatase alcalina foram encapsuladas em nanopartículas de PCL e entregues em células HeLa. Pretendeu-se também modular mecanismos celulares, tais como o stress oxidativo e a apoptose, com nanopartículas de PCL.

A absorção (por endocitose) por células HeLa de nanopartículas de PCL contendo enzimas encapsuladas foi seguida usando um corante vermelho fluorescente, a rodamina, que permitiu análises e medições por microscopia de fluorescência e citometria de fluxo.

Realizaram-se ensaios enzimáticos e celulares para medir a atividade da superóxido dismutase (SOD), após entrega enzimática por nanopartículas de policaprolactona. A produção de peróxido de hidrogénio intracelular foi detetada com um corante verde fluorescente, na presença de 30 µg/ml de lipopolissacárido (LPS). No entanto, os resultados obtidos não foram conclusivos devido a contaminação bacteriana ocorrida durante a síntese das nanopartículas. Foram igualmente realizados estudos por citometria de fluxo e ensaios de viabilidade celular. Os resultados indicaram que nanossistemas PCLSOD protegem as células HeLa do stress oxidativo, aumentando a viabilidade celular.

Para a fosfatase alcalina (ALP) observou-se que o encapsulamento em nanopartículas poliméricas de policaprolactona protegeu a atividade enzimática em solução. A análise por microscopia de fluorescência com o substrato Naftol AS-MX revelou o transporte eficiente de nanopartículas PCLALP para o meio intracelular.

Palavras-chave: nanopartículas de policaprolactona, nanoprecipitação, superóxido dismutase, fosfatase alcalina, stress oxidativo, apoptose.

ABSTRACT

The present thesis aimed at the development of polymeric nanoparticles as a vehicle for the delivery of enzymes into cells. The nanoparticles were prepared by nanoprecipitation of polycaprolactone (PCL) modified with propargyl 3-methyl pentanoate oxide. Superoxide dismutase and alkaline phosphatase were encapsulated in PCL nanoparticles and delivered into HeLa cells. Modulation of cell mechanisms, such as oxidative stress and apoptosis, with PCL nanoparticles, was also attempted.

The uptake (by endocytosis) of polycaprolactone-enzymatic nanoparticles by HeLa cells was followed using a fluorescent red dye, rhodamine. Rhodamine allowed analysis and measurements by fluorescence microscopy and flow cytometry.

Enzymatic and cellular assays were carried out to measure superoxide dismutase (SOD) activity in HeLa cells, after being delivered by polycaprolactone nanoparticles. Detection of intracellular hydrogen peroxide was performed with a cell-permeable green fluorescent dye in the presence of 30 μg/ml of lipopolysaccharide (LPS). However, the results obtained were not conclusive due to bacteria contamination during nanoparticle synthesis. Flow cytometry analysis and cell viability assays were also performed. The results indicated that PCLSOD nanosystems protect HeLa cells from oxidative stress, increasing cell viability.

For alkaline phosphatase (ALP), the encapsulation in polycaprolactone polymeric nanoparticles protected enzyme activity in solution. Analysis by fluorescence microscopy, using the fluorescent substrate Naphthol AS-MX disodium salt, revealed that PCLALP nanoparticles are successfully absorbed by HeLa cells.

Keywords: polycaprolactone nanoparticles, nanoprecipitation, superoxide dismutase, alkaline phosphatase, oxidative stress, apoptosis.

TABLE OF CONTENTS

LIST OF FIGURES

LIST OF TABLES

.

ABBREVIATIONS

Abs Antibodies

AKT serine/threonine kinase pathway

ALP Alkaline phosphatase

ALS Amyotrophic Lateral Sclerosis

BBB Blood-brain barrier

BCA Bincinchonic acid

BSA Bovine Serum Albumin

CAT Catalase

DLS Dynamic Light Scattering

DMEM Dulbecco's Modified Eagle Medium

ECM Extracellular matrix

ENSs Enzymes-loaded-nanosystems

EPT Enzyme Prodrug Therapy

ERK Extracellular signal-regulated kinases

ERK5 Extracellular signal-regulated kinases 5

ERT Enzyme Replacement Therapy

FBS Fetal Bovine Serum

FSC Forward-scattered light

GIT Gastrointestinal Tract

HIV Human Immunodeficiency Virus

JNK c-Jun N-Terminal Kinase pathway

LBP acute-phase LPS-binding protein

LPS Lypopolisaccharide

LPV Lipophilic drug Lopinavir

MAPK Mitogen-activated protein kinases

MRT Mean Retention Time

NIR near-Infrared

NP Nanoparticle

NPs Nanoparticles

PA Photoacoustic

PBS Phosphate-buffered saline

PCL Polycaprolactone

PDI Polydispersity Index

PLGA Poly(D, L-lactide co-glycolide)

PMPO Propargyl 3-methylpentonoate oxide

pNPP para-nitrophenyl phosphate

PTM Photomultipliers

ROS Reactive Oxygen Species

SOD Superoxide dismutase

SSC Side-scattered light

UV Ultraviolet

Chapter 1

1. INTRODUCTION

1.1 Motivation and Background

1.1.1 Enzymes delivery systems

Recently, enzymes have been used for many applications in the areas of health (i.e., enzyme replacement therapy), food (i.e., supplements), or in the environment (i.e., production of fuel). In medical applications, many enzymes are highly susceptible to denaturation, aggregation, or hydrolysis inside of the human gastrointestinal tract (GIT)[1]. To protect the proteins from these events, colloidal systems, composed by nanoparticles or microparticles, can be designed to encapsulate and deliver the enzymes[1]. For example, *Heyman MB et al. (2006)* developed a research work in the area of lactose intolerance in infants, in which they tested the oral delivery of lactase to perform the breakdown of lactose into galactose and glucose within the small intestine [2].

Molecular and physicochemical properties of the enzymes are essential details to be considered to design an optimum and capable colloidal delivery system for a specific application[1]. Proteins vary considerably in their molecular weights, conformations, electrical properties, polarities, and stabilities[1].

The dimensions and electrical characteristics of enzymes are important factors to determine the encapsulation properties of proteins in the delivery systems[1]. Size is strongly influenced by the aggregation state of the enzyme and its molecular weight that can vary depending on solution conditions, namely pH and ionic strength[1]. An enzyme to be encapsulated needs to be smaller than the hydrophobic domains of the delivering system[3]. The electrical properties are determined by the number of exposed anionic (-COOH<-> -COO + H+) and cationic (-NH_2 + H+ <-> -NH_3) groups on their surfaces that will strongly influence the release and retention of the active protein[1]. This

last property is weakened in the presence of salts due to electrostatic screening effects[1].

There are a variety of obstacles that need to be overcome so that the enzymes can be successfully delivered via oral route[1]. The oral route of enzyme administration can compromise the biological activity and stability of enzymes, mainly because proteins are highly susceptible to denaturation, aggregation, and hydrolysis when entering in contact with an acidic environment in GIT[4]. Also, the digestive enzymes, like proteases, present in mouth, and stomach can promote hydrolysis of proteins[1].

The low absorption of proteins within the GIT is accomplished due to the rheological properties of gastrointestinal fluids that will impact the mixing and transport of enzymes, thereby influence their residence time in GIT and their absorption rate[1,4]. When enzymes can be finally absorbed by epithelium cells, they face new challenges such as large size and polarity. This absorption can occur through a variety of mechanisms, like transcellular (passive or active), paracellular (T-junctions), and endocytosis, the one that will be the focus of the present study [1,5].

The optimum enzyme carrier system should protect the enzyme activity and be capable of encapsulating the number of proteins required to have the intended biological effect[5]. Some properties, such as thickness, composition, and charge of the interfacial layer can be controlled to control the retention and release of the enzyme[1].

One example of an enzyme delivery system, the one which is going to be used in this project, is nanoparticle (NP) systems. There are many ways to attach an enzyme in a nanoparticle surface, for example, it is possible to promote the insertion of cysteine residues in the enzyme, or also modifying NP's surfaces with nitrilotriacetic acid that will confer the surface a site to which histidine-tagged proteins can be readily attached[6]. *Feng Liu et al. (2015)* worked on the modification, by site-directed mutagenesis, of pyrophosphatase to create two mutants of SOD enzyme, with one residue of cysteine (Cys): MT1, with Cys residue near of active center and MT2, with Cys residue far from the active center, and both demonstrated a higher activity than the wild-type protein, 68.8%, and 91.2%, respectively[7]. The surface density of protein on the NP will affect its conformation state and, therefore, its reactivity with the targets. The random orientation

and weak binding associated with physical adsorption will make the surface density relatively low, leading to lower bioactivity.

Another way to promote the functionalization of nanoparticles (NPs) with enzymes is by introducing a mechanism of encapsulation, which is accomplished by means of weak chemical interactions such as ionic, and electrostatic interactions[8]. For example, polymeric NPs have been used mainly in medicine due to their generally small size and ease of synthesis. The NPs are capable of controlling the slow release of molecules of interest and protect drugs until they reach their local action[8].

A nanocapsule particle has core-shell morphology with an aqueous or oil cavity in which the active compounds are confined and surrounded by a polymer shell. Nanospheres have a matrix-like structure in which the active compounds and the polymer are uniformly dispersed[8]. As we want to conjugate an enzyme to these polymeric NPs, one way to control the enzyme release into the cell is by regulation of the rates of polymer biodegradation and the diffusion of the therapeutic molecule out of polymer matrix[8].

The delivery of enzymes into the intracellular medium provides a powerful tool for therapeutics[9], and it faces two significant barriers: an efficient cellular uptake and endosomal sequestration. One way to improve this uptake by the cells, with the maintenance of protein activity, is to conjugate the enzymes with polymeric NPs[9]. When we are working on drug delivery systems or enzyme delivery systems, we need to keep the efficient capping, the correct delivery, and release of the enzyme without losing its properties[8].

1.1.2 The scope of the thesis

The present master thesis is a research project to develop a practical and feasible carrier system for the delivery of enzymes into cells to modulate the cell functions. The carrier system will be the polycaprolactone (PCL) modified with propargyl 3-methyl pentanoate oxide (PMPO) that by nanoprecipitation synthesis mechanism will be

formulated into nanoparticles, which will encapsulate the enzymes superoxide dismutase and alkaline phosphatase, to deliver them into cells.

There are plenty of advantages to using enzymes as drugs to treat many types of diseases, and the reason that makes enzymes one of the best choices is the fact that enzymes bind and act on their targets with high affinity and specificity and converting target molecules into the desired products[10]. These reasons make them suitable agents for the treatment of many diseases such as lysosomal storage disorders, myocardial infarction, cystic fibrosis, tumor lysis syndrome, leukemia, and some collagen-based disorders such as Dupuytren's contracture[8].

When combining the enzyme therapy with nanotechnology, we are trying to create a system that works to overcome the barriers imposed against enzyme's action in the human body and create a more effective and straightforward way to be administrated.

Our study focuses on the activity of superoxide dismutase (SOD) and alkaline phosphatase (ALP), to deliver them into the cells, by encapsulating them into poly-caprolactone polymeric nanoparticles, without compromising their action and stability.

1.1.3 Organization of the document

The present thesis is organized into five chapters, in which the present introduction is the first chapter (Chapter 1). Chapter 2 includes the uptake of state of the art, which involves a bibliography review related to the topics presented, namely about cell functions, the enzyme delivery systems already implemented, and about nanotechnology in enzyme therapeutics. Chapter 3 describes the materials and methodologies that were used in the construction of the present work. In chapter 4, it is shown the results obtained, and discussion, for each one of the enzymes that were studied (SOD and ALP). Chapter 5 presents the main conclusions of the thesis and future perspectives. The thesis also includes an appendix with some results obtained regarding the characterization of PCL NP systems.

Chapter 2

2. STATE OF THE ART

2.1 Cell Functions

The cells are the unit of life responsible for the growth of all living organisms, due to their capability of reproduction and programmed death; they have their survival and error reparation mechanisms to secure the homeostasis of the living being[11]. To maintain their functions such as metabolization of nutrients, synthesis of macromolecules, or self-replication, cell's capabilities are defined by a dynamic rearrangement of biomolecules to achieve control and specificity[11]. One of the most important examples of their performances is the DNA repair mechanism, which ensures the correct replication of DNA to the next generation of cells and prevents some complicated diseases, such as cancer[11]. The cell's functions are determined by a network of nodes, for example, protein-protein; protein-DNA; protein-RNA, and protein-metabolites.

The functions and characteristics of the cells are stored in genetic information, in DNA molecules[11]. Through the DNA flow information mechanism, cells are capable of expressing their functions and play an important role in heredity[11]. The flow of genetic information is divided into two steps, the first one is the transcription in which the DNA molecule is converted in messenger RNA, and then the second step, translation, where RNA molecule is converted into its respective protein. Besides this flow of information, the cells are programmed to die by a mechanism known as apoptosis, to maintain the life of living organisms, and at any time that occurs some error during DNA replication or translation, to prevent some diseases to the organism[11].

Apoptosis can be useful for the cell, but can also be harmful, depending on the state of development of the tissue in the body[11]. Two major events compensate each other: cell proliferation, in which the cells replicate and replace older ones, and apoptosis. To induce cell proliferation, the system needs cell death-inducing genes, like the ones that codify for caspases. And so, apoptosis-induced proliferation is beneficial for the

organism, as it allows tissues to easily eliminate damaged or potentially dangerous cells and replace them with new and healthy ones[11]. In mammalian cells, apoptosis is controlled by the mitochondria pathway, which is mediated by caspases[11].

2.2 Nanotechnology in the modulation of cell functions

The functions of a cell are highly conserved and controlled by many types of mechanisms, but sometimes perturbations occur, which damage the cell environment and compromise the organism's stability. Medicine and technology have been evolving to give a better response to these perturbations using more simple, easy access and smaller systems that can act in our body with high efficiency. An area that leads with these types of systems is the so-called nanotechnology area. Cell biology area is tightly involved with nanotechnology to produce new experimental techniques not only to emulate more complicated, *in vivo*-like extracellular environments but also to monitor dynamic complex biological processes in real-time at the cellular level[11,12].

Cellular processes, such as adhesion, migration, and proliferation, are influenced by the chemical composition and morphology of the extracellular environment through interactions between cells and physical stimuli. The design of nanosystems for imaging and therapeutic applications requires an understanding of the interactions between NPs and those biological systems[11,10]. The extracellular factors, like growth factors, chemokines, and cytokines and interactions with the extracellular matrix (ECM), are expressed in a specific way and integrated by cells to initiate signaling cascades leading to the activation of cellular processes[9].

Advances in cellular and molecular technologies have made it possible to understand a vast range of cellular and molecular mechanisms, due to the unique properties of nanomaterials, they have plenty of advantages to be used in bioimaging diagnostic and therapeutic processes[11,12]. Nanostructures can passively interact with cells and mediate cell functions, as are recognized as objects that have a dimension ranging that enhances their activities in the living organism because some of the materials can mask the action of the immune system that will not recognize them[12]. Nanomaterials have

increased surface to volume ratio compared with their bulk materials, and this will increase mechanical strength, to enter through cell barriers[10].

Nanomaterials can be designed to act as ECM to present a combination of chemical, mechanical and biological factors that provide required signals to direct cell fate[13]. When they cross cell barriers, they can bind to specific biological targets, such as ligands, proteins, antigens, or cell types. Examples of these nanostructures are gold nanoparticles, semiconducting (CdSe, CdS, ZnS), magnetic (Fe_3O_4), and polymeric nanoparticles[11].

Polymeric nanoparticles can be made with natural polymers, that are good carriers for drug delivery systems because of their wide sources, better stability, low toxicity, simple mild preparation methods, and versatile routes of administration. Synthetic polymeric nanoparticles have been widely applied in cancer therapy due to flexibility in designing and modifying their compositions and structures[9].

Another cell property that can be manipulated with nanostructures is cell alignment. Several groups have developed nanoporous surfaces and the results showed that after the treatment with nanoporous the cells present a high degree of alignment when compared to the normal ones[9].

2.3 Enzymes as therapeutic agents

There are plenty of advantages of using enzymes as drugs to treat many types of diseases such as lysosomal storage disorders, myocardial infarction, cystic fibrosis, tumor lysis syndrome, leukemia, and some collagen-based disorders such as Dupuytren's contracture[8].

In terms of the usage of enzymes for cancer treatment, it is used PEGlyated arginine deaminase, an arginine-degrading enzyme, that can inhibit human melanoma and hepatocellular carcinomas, which are auxotrophic for arginine owing to a lack of arginosuccinate synthetase activity[11]. Another type of drug enzyme is the PEGylated asparaginase that has great efficiency in the treatment of leukemia. Whereas normal cells can synthesize asparagine, cancer cells cannot and die in the presence of this

asparagine degrading enzyme[7]. Some other types of enzymes can act in proliferation that promotes uncontrolled growth of the cells, like chondroitinase A and chondroitinase B that will inhibit tumor growth, neovascularization, and metastasis[7].

Prodrugs are derivatives of therapeutic agents designed to enhance the pharmacokinetic profile of the drug. When is used this concept, we are overcoming some limitations imposed by regular drugs, which are poor aqueous solubility, poor absorption from the gastrointestinal tract, and poor rates of cell delivery[7]. One of the areas of prodrug development is enzyme prodrug therapy (EPT), where a specific enzyme will perform the step of bioconversion in prodrug degradation. The main goal in EPT is to achieve a site-specific drug recovery, by using a set of techniques like antibody-directed enzyme prodrug therapy[7].

Poor solubility is considered as a serious problem limiting the therapeutic use of numerous drugs and drug candidates, a problem which prodrugs research field is trying to overcome[13,14].

The present study focuses on the so-called enzyme replacement therapy (ERT) field. Enzyme therapy is a medical treatment that consists of the replacement of the defective enzymes in the human organism, by giving the patient a solution containing the enzyme, which can be accomplished by oral or intravenous routes[15]. This concept can be used for the treatment of a variety of diseases such as lysosomal storage diseases, first enunciated by Christian de Duve in 1964. This therapy can replace a defective or absence enzyme in the human system and allows to understand better the correlation between endocytosis and lysosomes, possibilities the treatment of many diseases, but it has many hurdles to be overcome such as poor solubility, poor stability of the enzyme in GIT (in case of oral administration)[15].

Despite many beneficial outcomes of ERT, several limitations such as the high cost of the treatment and various inadvertent side effects (e.g., immunological responses) against the infused enzyme and development of resistance to enzymes persist[16]. Neutralizing antibodies (Abs) can reduce the efficacy of ERTs via direct interference with the enzyme activity because they can interact with the active site of the enzyme and/or ligands involved in the binding to a receptor on the target cells. Due to this limitation of ERT, enzymes-loaded-nanosystems (ENSs) have been developed using

advanced nanomaterials to increase the efficacy of the treatment while minimizing the side effects[16]. A large variety of nanocarriers can be used for this goal, like biodegradable nanomicelles, nanoliposomes, and polymer-and lipid-based nanoparticles[16].

2.4 Superoxide dismutase approach

2.4.1 Origin and structure of superoxide dismutase

SOD is an enzyme ubiquitous among aerobic organisms, that protects the living being from oxidative stress, produced by reactive oxygen species that specifically catalyzes the dismutation of the superoxide anion ($O_2^{\cdot-}$) to H_2O_2 and O_2[17]. Through sequencing, alignment, and phylogenetic analysis several primitive antioxidants were examined, leading to the identification of three primary ROS removal enzymes: SOD, catalase (CAT), and peroxiredoxins (PRDX). The SOD families are defined by the metal ions utilized for stability and catalysis, dividing SOD into four different families, Cu/Zn, Ni, Mn, and Fe SODs, in which Cu/Zn SOD is generally homodimeric and is present in diverse locations of different organisms[17,18]. The most primitive enzyme's family are the Fe- and Mn-SODs, the most ancient form of SOD that is found in both aerobic and anaerobic bacteria[18]. FeSOD has also been identified in Archaea, Protists, and even eukaryotic plants, providing evidence not only to the prolonged existence of this SOD isoform but also the versatility[18].

The SOD used in the present study is CU/Zn SOD from bovine erythrocytes, which is a metalloprotein with a molecular weight of 32 kDa. It is a homodimer enzyme with one copper (responsible for enzymatic activity) and zinc ion (responsible for structural stability) per subunit and has an antiparallel "greek-key" β barrel fold[18]. This SOD isoform is a member of the second family of SODs, the most modern family of the SOD lineages[19]. The CuZN-SOD is ubiquitous among plant and animal species and is localized in the nucleus, cytoplasm, mitochondrial intermembrane, chloroplast, and even in bacterial, especially in gram-negative bacteria.

Figure 1 – Model of Cu/Zn SOD. The metal ions are represented in brown: Cu^{2+} and in grey: Zn^{2+}. Adapted from UniProt.org

One of the first reports on superoxide dismutase appeared in 1939, during a research work developed by *Mann and Kellin* [21], where they isolated a blue copper protein from bovine erythrocytes named erythrocuprein, which had no enzymatic activity[21]. The SOD enzyme as we know now was discovered by *Irwin Fridovich* in 1969, a research work that led to the proposal of an enzyme that catalyzes the dismutation of superoxide free radical anions[22].

2.4.2 Superoxide dismutase roles in cells

Reactive oxygen species (ROS) are extremely reactive oxygen-containing molecules produced during oxygen metabolism within the cells, but sometimes, they can cause oxidative stress when reacting with and damaging intracellular targets, such as lipids, proteins, and DNA[17]. In eukaryotic cells, ROS are generated in metabolic processes during mitochondrial respiration. At physiological levels, ROS are important modulators of many cellular functions from metabolism, signal transduction to stress responses, and their levels are controlled by the antioxidant system of the body[17]. The enzyme SOD is one of the major proteins of this system, by converting $O_2^{\cdot-}$ into H_2O_2 and O_2, which is represented in the following chemical reaction:

$$2O_2^- + 2H^+ \rightarrow H_2O_2 + O_2 \quad \text{(Eq. 1)}$$

The hydrogen peroxide is further converted into harmless products such as water, by other enzymes like catalases and peroxidases[17]. The precursor molecule of superoxide anion is the molecular oxygen, an ideal electron sinks which are, in biology, the final electron acceptor in oxidative metabolism[18]. This process is established in mitochondria, where occurs the production of ROS[23]. Molecular oxygen is the optimum electron acceptor since in its fundamental state it poses two unpaired electrons whose standard biological conditions energetically favors the reduction of O_2 by one-electron transfers[18,23]. To prevent toxic levels of superoxide anion (above 200 pM[18]), the living organisms generated ROS-detoxifying enzymes, like superoxide dismutase. Molecular oxygen can be beneficial for many molecular pathways, such as oxidative phosphorylation in the mitochondria to generate water, but the oxidizing nature of O_2 may also contribute to the uncontrolled pathological removal of electrons, leading to the damage of vital cellular components and the generation of ROS[18].

Two major cell signals will activate the ROS-generation mitochondria pathway: when the mitochondria are not making ATP and consequently has a high protonmotive force; and when there is a high NADPH/NADP+ ratio, that will activate the enzyme NADPH oxidase enzyme, the one responsible for producing of superoxide anion[23].

Besides its natural roles, superoxide dismutase has important action in several human diseases. It is known that the mutations in the SOD gene, can have an impact in amyotrophic lateral sclerosis (ALS) and respiratory diseases[17]. ROS-induced oxidative stress has been established as an implicated pathophysiology in several conditions, such as aging, infertility, cardiovascular diseases, and neurological disorders[24].

In amyotrophic lateral sclerosis, the Cu/Zn SOD is associated with this disease[18]. The majority of Cu/Zn SOD mutants in ALS possess equal or higher amounts of intrinsic activity[25], this arguing one of two things: 1) CuZnSOD mutations leading to ALS are not dependent upon SOD activity-based but more on specific properties of the protein; or 2) the mutations caused differential localization of CuZnSOD leading to aberrant or deficient ROS signaling cascades[18,25].

SOD has also an important role in cancer events. ROSs are excessively accumulated inside the cells in cancer situations, due to the aberrant cell metabolism[26]. There are three major types of SODs involved in cancer; SOD1, SOD2, and SOD3. The SOD1 was extensively studied in the field of neurodegenerative diseases but recently was also found to have a paradox role in cancer development. On one hand, when the levels of SOD1 decrease there is an increment in ROS levels, which will cause oxidative DNA damage and promote carcinogenesis. But, in another hand, cancer cells have a high content of oxygen reactive species, which is increasingly dependent on activated antioxidants, such as SOD1[26]. Malignant cells have high levels of ROS, which leads to an increase of oxidative stress response and upregulation of antioxidant systems, like SOD 1[26].

Finally, SOD also plays an important role in a disease called emphysema, which involves the generation of oxidative stress and alveolar cell apoptosis[27]. Oxidative stress upregulates ceramides, proapoptotic signaling that trigger further oxidative stress and alveolar space enlargement. And to model, the direct lung effects of ceramides, a treatment with superoxide dismutase was applied to prevent the growth of emphysema[27]. As a result, Cu/Zn SOD overexpression prevented ceramide-induced lung oxidative stress[27].

2.4.3 Nanotechnology applications of superoxide dismutase

SOD has attracted wide research interest because the electron transfer mechanism between the substrate and the enzyme active site is considered to have reached perfection and because the enzyme shows unusual stability to urea, high temperatures, and prolonged refrigeration[17]. Although SOD is a potent antioxidant, there have been several attempts to further improve its activity, because it is limited by diffusion. To overcome the barriers of antigenicity, stability, and pharmacokinetics, SODs can be functionalized with nanocarriers such as liposomes, gold nanoparticles, or polymeric nanoparticles[28]. For example, in Alzheimer's disease, a Mn(II)-based superoxide dismutase mimic was developed as a prodrug candidate to target Cu(II) associated

events, because of divalent copper ions can induce the formation of reactive oxygen species and modulate the amyloid peptide aggregation[26].

Kost O.A et al. (2016), developed a research project in the area of ocular inflammatory disorders, based on the creation of a system called “nanozyme”, which uses an electrostatic coupling between SOD1 and a cationic block copolymer[28]. When infected cells are treated with SOD1, they showed anti-inflammatory activity, however, the “nanozyme” was much more effective compared to the free enzyme. These results support the idea that polymeric nanoparticle systems offer better biocompatibility and adhesiveness that will possibilities the drug to overcome the corneal diffusion barrier[28]. These “nanozyme” are NP systems that exhibit the properties of an enzyme and they offer several advantages over natural enzymes[29].

The work carried out by *Maram K.Reddy et al*. (2008), showed a polymeric nanoparticle system made by poly(D, L-lactide co-glycolide) (PLGA) and SOD enzyme capable of protection of neurons against hydrogen peroxide-induce oxidative stress[30].

The delivery of drugs or therapeutic enzymes has been challenging primarily because of the tight junctions between the brains’ endothelial cells that form the blood-brain barrier (BBB) [30]. When encapsulating the enzyme SOD into PLGA nanoparticles, this polymer is compatible with human neurons, and so it promotes the uptake of brain cells for SOD enzyme and stimulates its action on the brain diseases, such as Alzheimer's or Parkinson disease[30]. The results of this work showed that when SOD is conjugated with PLGA nanoparticles (NPs) presented an increase in half-life time in vivo and permeability across the cell membrane[30].

2.5 Alkaline phosphatase approach

2.5.1 Origin and structure of alkaline phosphatase

Phosphatases are enzymes that catalyze the hydrolysis of esters from phosphoric acid with the release of inorganic phosphate[31]. They occur in cells and extracellular fluids and are mainly represented by acid phosphatase (active in an acid pH, 4.8 pH) and alkaline phosphatase (active in an alkaline pH, 9.8 pH) [31].

ALP is a homodimeric enzyme and a membrane-bound glycoprotein that catalyzes the hydrolysis of phosphate monoesters. It has a molecular weight of 86 kDa and the active site region contains three metal ions, two zinc, and one magnesium ion, that are fundamental for the enzymatic activity[31].

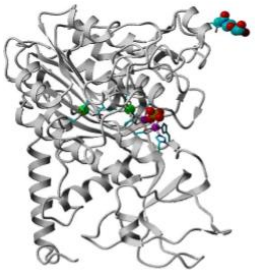

Figure 2 – Model of mammalian alkaline phosphatase, with the metal ions in the active center: magnesium is represented in green, and zinc is represented in magenta. Adapted from UniProt.org

The human genome encodes four isoenzymes of ALP, tissue-specific, that are intestinal ALP, placental ALP and germ cell ALP, and tissue non-specific ALP, that are present in the liver, bone, and kidney[31]. Serum ALP activity is used as a diagnostic indicator of several human diseases, like bone and liver diseases[31].

One of the first reports on ALP appeared around 1912 when *Grosser & Husler* suggested that phosphatases are present in a variety of tissues and could hydrolyze glycerophosphate and fructose 1-6 diphosphate in intestinal mucosa [31]. In nature, ALP is found in both eukaryotic and prokaryotic organisms. It is present in bacteria, fungi, and mammals[32].

2.5.2 Alkaline phosphatase roles in cells

The knowledge of the biological functions of alkaline phosphatases was carried out by Robinson, which demonstrated that this enzyme plays an important role in ossification since during this event there is an increase in the concentration of inorganic phosphate thus to deposition of bone salt[33].

In mammals, the role of ALP in ossification can be divided into two: 1) responsible for the precipitation of calcium phosphate, due to the high concentrations of inorganic phosphate and 2) allows crystal growth at nucleation sites. In the intestine and kidney, due to the high concentrations of ALP, the enzyme has a direct role in the transport of nutrients across the epithelial membrane[34].

Also, ALP plays an important role in the regulation of protein phosphorylation, cell growth, cellular migration during embryonic development, and in apoptosis[35]. Apoptosis, the process in which the cell dies, is an event regulated by a myriad of intracellular molecular pathways, as above described, with many involving protein phosphorylation and dephosphorylation[35]. In eukaryotes, the phosphorylation typically occurs on three amino acid residues: serine, threonine, and tyrosine. Apoptosis is an energy-dependent process associated with morphological changes including cell cleavage, shrinkage, chromatin condensation, and DNA fragmentation. And all of these processes depend on proteins that are regulated by phosphatases[35].

The apoptosis mechanism it is split into two major pathways: the intrinsic pathway (mitochondria signal pathway) and the extrinsic pathway (death receptor pathway), both mechanisms are closely related to[36]. In the mitochondria regulated pathway, phosphatases play important roles in the mediation of signals that arise from ion channels. Ion channels are integral membrane proteins that mediate the efflux/influx of essential signaling ions into/from the cell thereby controlling cytoplasmatic ion concentrations, membrane potential, and cell volume[36].

The calcium ion channel it is closely related with the mitochondria intrinsic pathway, in this mechanism, the increase in calcium (Ca^{2+}) concentration in the cytosol induces the uptake of mitochondria for calcium, and it is responsible for the activation of an important enzyme, phosphatase enzyme, the Ca2+-activated protein phosphatase calcineurin, that dephosphorylates the BCL-2-associated agonist of cell death (BAD), a pro-apoptotic member of the BCL-2 family, thus enhancing BAD heterodimerization with BCL-XL and promoting apoptosis[36].

The B-cell lymphoma 2 (Bcl-2) family proteins are central regulators of cell death and are divided into two classes, multidomain proteins that are either pro or antiapoptotic and present similarity in three or four regions. And the proapoptotic interacting-domain

death agonist (BH3)-only proteins that are homologous in only a single region[37]. These proteins are responsible for the first regulatory step of the mitochondria apoptosis pathway.

Proapoptotic multidomain proteins (Bcl-2-associated proteins, Bax, and Bak) act at the mitochondrion and are essential for the cell death process. Upon activation, they homo-oligomerize to release factors such as cytochrome c that will interact with apoptotic protease-activating factor 1 (Apaf- 1) to initiate a proteolytic caspase cascade that executes apoptosis through cleavage of cellular protein[36,38]. Antiapoptotic multidomain (e.g., Bcl-2) inactivate pro-apoptotic proteins by binding their amphipathic α-helical BH3 region via a hydrophobic cleft. The BH3 proteins act as sensors for cellular stress and initiate cell death by either directly activating Bax and Bak or by disrupting the connection between proapoptotic and antiapoptotic multidomain family members[36].

ALP and other enzymes can be utilized for effective enzyme-replacement therapy for some lysosomal storage disorders (Gaucher, Fabry, and Pompe diseases), for myocardial infarction and tumor diseases[31].

Phosphatases play important roles in pathways involved in cell death, like serine/threonine kinase pathway (AKT), mitogen-activated protein kinases (MAPK), and DNA damage response [35]. The AKT pathway is important in the transduction of signals of growth factors and other extracellular stimuli to regulate cell growth, survival, and death. Serine/threonine-protein is phosphorylated at multiple sites and its activation promotes cell survival[35]. Phosphatases can modify the molecular components of the apoptosis, like caspases[35].

2.5.3 Nanotechnology applications of alkaline phosphatase

The enzyme ALP has been applied in the nanotechnology research field in the area of photoacoustic (PA) imaging[39], which is important for the diagnosis of superficial cancer with high spatial resolution. *Chengfan Wu et al. (2018)*, created an ALP-

activatable near-infrared (NIR) PA nanoprobe, which upon ALP dephosphorylation, self assembles into nanostructures with increased PA signal for tumor imaging[39].

In the tumor microenvironment, 1P (PA nanoprobe) will be dephosphorylated by the secreted ALP to yield a more hydrophobic product IR775-Phe-Phe-Tyr-OH, which is uptake by tumor cells and self-assembles into nanoparticles (1-NPs) [39]. Formation of 1-NPs will induce the self-quenching of the NIR fluorescence but in the meantime enhancement of the PA signal for tumor imaging[39].

Another application of ALP is in the orthopedics research field[40]. There have been developed nanophase materials as bone implants to overcome the limitations applied by the regular implants, such as, poor initial bone growth on the surface of the implant; generation of wear debris in articulating components of implants that become lodged between the implant and surrounding tissue; and stress and strain imbalances between an implant and surrounding tissue that leads to implant loosening[40].

ALP can also have a usage in colorimetric immunoassays for tumor marker detection[41]. Nanomaterials-based colorimetric immunoassays are an excellent alternative against the regular enzymatic immunoassays since nanomaterials can amplify the signal because they can catalyze chromogenic reactions, due to the presence of artificial enzymes[41]. Due to the intrinsic catalytic properties of ALP, the enzyme has usually been adapted in biomedical-related assays as a signal amplifier. The detection principle is related to the oxidation of a substrate under the catalysis of a natural enzyme. The change of signal intensity is linear with the target concentration, allowing an easy detection[41].

2.6 Polymeric nanoparticle systems for delivering of enzymes into cells

NPs are solid colloidal particles with diameters in the nanometer range. They consist of macromolecular to even smaller range materials such as polymeric nanoparticles, lipid-based carriers, dendrimers, and gold NPs[42]. Polymers are the most common materials for generating NPs drug carriers, because of their ease of synthesis, low cost,

biocompatibility, and biodegradable capabilities, non-immunogenic and non-toxic properties[42,43].

Polymeric NPs can be generated from natural polymers, such as chitosan or by synthetic polymers like polyesters poly-caprolactone or monomers polymerized *in situ*, poly-akylcyanoacrylate[43]. Some polymers like poly-caprolactone have the capability of biodegradation, which makes them suitable for many diseases treatment, for example, cancer, and that is the reason why they present reduced toxicity and do not accumulate in the cells after administration[42].

Both drugs delivery and nanomaterials fields are facing new challenges, they need to overcome the limited effectiveness of the drug, the poor absorption, and the undesirable side effects due to the lack of sensitivity[43]. Nanomaterials are a good solution that allows the overcome of these issues, but at the same time they have a large-scale production challenge and there is a need for scale-up laboratory technologies for the commercialization part[43]. The major function of the carrier system is to deliver the pharmaceutical agent to a specific site of action, achieving a higher concentration of therapeutic agents and increasing its effectiveness and efficiency[44].

The polymer that is going to be studied in this thesis is PCL, which is a semi-crystalline biodegradable, biocompatible, and hydrophobic polyester with low glass transition temperature and melting point[45]. It is also non-toxic and non-mutagenic[45,46]. It has the lowest degradation rate of all the common polymers which makes PCL suitable for delivering drugs for chronic therapy[45]. One research work that used PCL as a nanocarrier, was carried out by *Punna Rao Ravi et al*., in which they entrapped lipophilic drug lopinavir (LPV) for the treatment of Human immunodeficiency virus (HIV)[45]. Following the oral administration, polymeric NPs showed statistically significant improvement in the pharmacokinetics of LPV, and an increase in its mean retention time (MRT)[45].

The stability of the polymers usually depends on their molecular weight, the crystallinity of the polymer, and the pH of the solution. *D. Lemoine et al*. studied the stability conditions of three polymers: poly-caprolactone, poly(D, L-lactide) and poly(D, L-lactide-co-glycolide), in which PCL was the most stable one[47]. The stability depends

on the storage temperature. PCL can be kept at 4ºC and room temperature during one year without compromising its activity[47].

The biodegradation property of PCL is affected *in vitro* by the preparation method of the delivery system; by polymer properties such as initial molecular weight and by physical and chemical parameters like temperature, pH, and ionic strength[47].

Chapter 3

3. MATERIALS AND METHODOLOGIES

3.1 Materials

Enzymes

A) Calf intestine alkaline phosphatase

The alkaline phosphatase, from bovine calf intestine, utilized during the enzymatic experiments was supplied by Promega. According to the supplier, the solution has an activity of 1000U/ml and is supplied in a solution containing 10mM Tris-HCl (pH 8.0), 1mM $MgCl_2$, 0.1mM $ZnCl_2$, 50mM KCl and 50% (v/v) glycerol.

B) Cu/Zn Superoxide dismutase from bovine erythrocytes

The Cu/Zn Superoxide dismutase, from bovine erythrocytes, utilized during the enzymatic experiments was supplied by Sigma Aldrich. According to the supplier, the solution has an activity of 3000U/mg protein.

Reagents

The main chemicals used during this research project are listed in Table 1.

Table 1 - Reagents utilized during the experiments

Chemical	Supplier	Purity
Acetone	VWR Chemicals	99.8%
Rhodamine octadecyl ester perchlorate	Sigma Aldrich	98%
Trizma base	Sigma Aldrich	98.9%
Magnesium chloride ($MgCl_2$)	Sigma Aldrich	98%
Zinc Chloride ($ZnCl_2$)	Sigma Aldrich	98%
Dichloromethane	Sigma Aldrich	99.9%
Chloroform	VWR Chemicals	99.8%
Naphthol AS-MX phosphate disodium salt	Chemcruz	98%
p-nitrophenyl phosphate (pNPP)	Roth	99%
MTS reagent	Abcam	98%
DMEM-10% of fetal bovine serum	Invitrogen	-

Trypsin 0.25%-EDTA	Pan Biotech	-
Rhodamine octadecyl ester perchlorate	Sigma Aldrich	98%
HeLa cells	Invitrogen	-

Methodologies

3.2 Enzymatic Assays

3.2.1 Quantification of protein concentration BCA-Protein assay

The bicinchoninic acid (BCA) assay was performed to quantify the proteins encapsulated in the nanoformulations synthesized, by the nanoprecipitation method. The method of BCA is based on the chelation of Cu^{+} ions by two molecules of bicinchoninic acid[48]. The reaction is divided into two steps: first, the peptide bonds in protein reduce Cu^{2+} ions from the copper(II) sulfate to Cu+ (a temperature-dependent reaction). The amount of Cu^{2+} reduced is proportional to the amount of protein present in the solution, and second, the two molecules of bicinchoninic acid chelate with each Cu^{+} ion, forming a purple-colored complex that strongly absorbs light at a wavelength of 562 nm[48].

This assay was performed with a range of SOD and bovine serum albumin (BSA) proteins concentrations of 0-1 mg/ml and 0-2 mg/ml, respectively. This is an important step because, like this, it was possible to verify if the standard method (the one done with BSA protein calibration curve) is suitable enough for SOD quantification, or it requires a separate calibration curve. The assay was performed in a 96-well microplate using BCA reagent (Reagent A and Reagent B in a proportion of 50:1) supplied by Thermo Fischer, incubating the microplate at 37ºC for 30 minutes. The absorbance was measured in a microplate reader (BioTek, synergy h1 at 562 nm.

3.2.2 Intracellular hydrogen peroxide detection assay

Hydrogen peroxide is a reactive oxygen species produced through the metabolism of molecular oxygen, which serves as both an intracellular signaling messenger and a source of oxidative stress. The compound is generated in cells via multiple mechanisms such as the NOX-mediated ROS production by neutrophils and macrophages or by the dismutase of superoxide anion, by SOD enzyme. This assay was performed to verify the SOD activity (but not in quantitative terms) after being encapsulated and delivered into HeLa cells.

The kit used to test the presence of H_2O_2 was ordered from Sigma Aldrich [49] and provides a method to detect hydrogen peroxide in living cells. The kit utilizes a cell-permeable sensor that generates a fluorescent product (ex/em=490nm/520nm) after reaction with intracellular H_2O_2 that can be analyzed by a fluorescence microplate reader or flow cytometry.

To verify the presence of hydrogen peroxide in HeLa cells it was required the generation of ROS in cells. This production of H_2O_2 is accomplished using lipopolysaccharide (LPS). Lipopolysaccharide is a compound of the outer membrane of gram-negative bacteria, such as *Escherichia* and *Salmonella* species[50]. The molecule consists of lipid A (endotoxin) which is responsible for the toxic proinflammatory properties of LPS and polysaccharide side chain component, which consists of a core oligosaccharide, and the terminal O-specific chain antigen that determines the serological specificity or the bacterial serotype[50]. The infection caused by Gram-negative agents results initially in the stimulation of the nonspecific immune response mediated by tissue inflammatory cells such as monocyte, neutrophils, and polymorphonuclear leukocytes[51]. When these cells are activated, they can contribute to the generation of inflammations by producing mediators such as cytokines and ROS[51].

When LPS enters in the host organism, first become in contact with its binding protein, the acute-phase LPS-binding protein (LBP) in the plasma[52]. This first step will activate two types of responses, the non-specific immune response (activation of leukocytes and macrophages) to try to kill the bacteria, and the specific-immune response that will activate the transcription factors responsible for the activation of NADPH oxidase[51,52]. After transcription factors are activated, they will up-regulate the assembly of NADPH oxidase, they will increase the level of Rac 2, a small GTP-binding protein associated with $p47_{phox}$ and $p67_{phox}$. When the levels of Rac 2 increase it will stimulate the translocation of cytosolic factors and Rac 2 to associate with flavocytochrome b_{558}, thereby assembling the active O_2-generating complex[51].

Both these responses generate in the end a high level of ROS in the cells, so it will activate some signaling pathways, including the kinase-nuclear factors pathways and MAPK pathways, that will lead to the cell death[52].

The assay was performed by seeding 75000 cells/well in a 48-well microplate in the presence of 30 µg/mL of LPS. The plate was incubated overnight in an incubator at 37ºC with 5% (v/v) of CO_2. After incubation, the medium was replaced by *Dulbecco's Modified Eagle Medium* (DMEM) without phenol red, and the nanoformulations: 50 µl PCL, 50 µl PCL_SOD into 200 µl of DMEM without phenol red, and free 0.2 mg/mL of SOD were added into each well, following incubation of 4h, at 37 ºC.

3.2.3 Alkaline phosphatase activity in solution: *p*-nitrophenyl phosphate activity assay

Alkaline phosphatase activity can be measured using the substrate *p*-nitrophenyl phosphate (pNPP), that after hydrolyzed by ALP will be covert into a water-soluble yellow product (*p*-nitrophenol), with strong absorption at 405 nm[53].

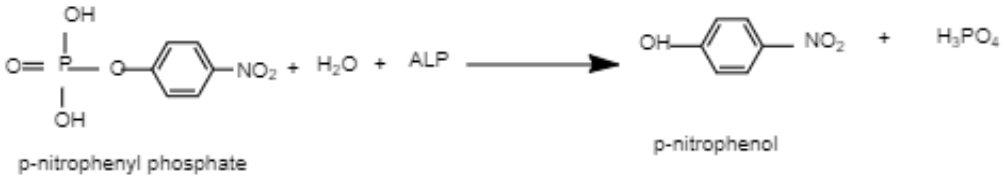

Figure 3 – *p*-nitrophenyl phosphate hydrolysis by ALP.

The buffer used in this assay was 50mM Tris-HCl pH 8.0, with and without the addition of 1mM of $MgCl_2$ and 0.1mM of $ZnCl_2$ metal ions. The assay was performed in a 96-well microplate by preparing 5mM of pNPP and mixed with 10 µl of ALP (free ALP and PCLALP NPs) into each well, at 25ºC and 37ºC during 60 minutes, to verify if the temperature could influence the ALP activity. The absorbance was measured in a microplate reader, Biotek synergy h1.

The conversion ratio between the substrate *p*NPP phosphate, which absorbs at 370 nm, and its product *p*-nitrophenol which absorbs at 405 nm was calculated by the following equation

$$\frac{A405}{A370} = \frac{Abs(405nm)}{Abs(370nm)} \qquad \text{(Eq 2)}$$

This ratio was important to verify the capability of substrate conversion by ALP free in solution and encapsulated in PCL NPs.

3.2.4 Alkaline phosphatase activity assay in cells: Naphthol AS-MX disodium salt activity assay

The assay with naphthol AS-MX disodium salt was performed to verify the activity of ALP in HeLa cells, after being delivered by PCL NPs. The naphthol phosphate derivates, like the one that was used, is a non-fluorescent compound, with a molecular weight of 415.29 Da, that after hydrolysis by ALP becomes red fluorescent with an emission/excitation wavelength of 388nm/512 nm, between pH 8.0 and pH 9.0[54,55].

The assay was carried out in a 48 well-microplate by seeding 75000 cells/well, with an overnight incubation at 37ºC with 5% (v/v) CO_2 incubator. In the day after, the cells were washed x1 with phosphate-buffered saline (PBS) and the medium was replaced by a new DMEM. The nanoformulation (10 µl of PCLALP in 200 µl of DMEM, with different amounts of ALP) were incubated in cells for 4 hours at 37ºC. After incubation, a concentration of 5mM of naphthol AS-MX disodium salt (dissolved in DMEM without

phenol red) was added into each well and was incubated for 45 min at 37ºC. In the end, the fluorescence intensity was measured in a microplate reader Biotek synergy h1, flow cytometry, and the cells were observed in fluorescence microscopy.

3.3 Synthesis and characterization of polymeric nanoparticles

3.3.1 Nanoprecipitation

Nanoprecipitation is a technique based on the interfacial deposition of a polymer after the displacement of the organic solvent from a lipophilic solution to the aqueous phase. It is a one-step procedure for polymeric nanoparticle synthesis, which means that is a method that does not need an emulsification step before the generation of NPs[56]. The polymer that was used in this thesis was polycaprolactone (with propargyl 3-methyl pentanoate oxide, PMPO) 2.5 mg/ml dissolved in acetone. The nanoprecipitation technique is based on the interfacial deposition of a polymer after the displacement of the organic solvent from a lipophilic solution to the aqueous phase. The polymer PCL was dissolved in a water-miscible solvent (acetone) and this solution was added into a stirred aqueous solution in one shot. As the solvent diffuses out from the nanodroplets, the polymer precipitates in the form of nanocapsules or nanospheres[56].

In this thesis from 3.3.1 section until the end of the document the nanoformulations will be treated as PCL NP (for PCL NP), PCLSOD (for SOD encapsulated in polycaprolactone nanoparticle) and PCLALP (for ALP encapsulated in polycaprolactone nanoparticle).

After dissolving 2.5 mg/ml of PCL in 1ml of acetone, it was added the same volume of milli-Q water (1ml) in one-shot to synthesize the nanoparticle PCL NP. To synthesize the nanoformulations PCLALP and PCLSOD, ALP, and SOD enzymes were added in different concentrations to the aqueous phase (Milli-Q water 1ml). These enzyme solutions were then added to the organic phase (2.5 mg/ml of PCL in 1 ml of acetone), also in the one-shot procedure.

For the encapsulation of the SOD enzyme, it was incorporated the following concentrations: 0.02 mg/ml, 0.04 mg/ml, 0.050 mg/ml, 0.1 mg/ml, 0.2 mg/ml, 0.4 mg/ml, 0.5 mg/ml, and 1 mg/ml of SOD enzyme, in 1 ml of Milli-Q water each. After dissolving the enzyme in the Milli-Q water, the different 1 ml of SOD solutions were added to the PCL/acetone solution, in the one-shot procedure. To generate the nanoformulations PCLSOD, each solution was transferred to dialysis membranes (50 kDa) to initiate the dialysis step, which is performed overnight against 3l of distilled water, with continuous agitation, at room temperature.

In the case of nanoformulations encapsulating ALP enzyme, PCLALP nanoformulations, the following ALP concentrations were added: 0.98 µg/ml, and 9.86 µg/ml in 1ml of Milli-Q water. The dialysis step was performed at 4ºC and against Tris-HCl pH8 buffer (3l). Also, it was added the magnesium and zinc ions ($MgCl_2$ and $ZnCl_2$), in the 1ml of the aqueous phase, into each nanoformulations PCLALP. So, it was formulated 4 different PCLALP, two with a lower amount of ALP (0.98 µg/ml), in which one of them has 0.1 mM of zinc 0.1 mM, and 1mM of magnesium, and the other just ALP without ions. The other two, have a higher amount of ALP (9.86 µg/ml) and one of them has the same concentration of the zinc and magnesium ions as the PCLALP with a lower amount of ALP, and the other one just ALP without the metal ions.

It was also added an organic dye, rhodamine octadecyl ester perchlorate, a red fluorescent dye to enable the visualization of HeLa cells in fluorescence microscopy, after delivering of nanoparticles_enzymes systems. In PCLSOD and PCLALP nanoparticles, it was added an amount of rhodamine of 100 µl (Sigma Aldrich) in each one. To encapsulate this dye, it is necessary to add the 100 µl of dye in the 1ml of PCL/acetone solution, and only after this step it is possible to add 1 ml of ALP/Milli-Q or SOD/Milli-Q water solution.

3.3.2 Phase extraction and freeze-drying

The assays of phase extraction and freeze-drying were performed to characterize the nanoformulations generated, by the means of polymer and encapsulated enzyme quantification (mg/ml). Phase extraction is a method based on the separation of compounds that are dissolved in a liquid mixture, that have different physical and

chemical properties. To achieve this goal, two organic solvents were used: dichloromethane and chloroform. These two compounds will separate the nanoformulation solutions into the aqueous phase (water with enzyme) and the organic phase (organic solvent with PCL polymer).

Freeze-drying is a water removal process typically used to preserve perishable materials, to extend shelf life or make the material more convenient to be transported. It works by freezing the material (- 70 ºC), then reducing the pressure and adding heat (30 ºC) to allow the frozen water in the material to sublimate[57].

After adding 1.8 ml of each organic solvent into 1 ml of each nanoformulations, the organic phase (1ml) was collected into glass flasks, so it could be left to dry overnight and the aqueous phase (1ml) was collected into Eppendorf tubes of 1.5ml so it could be left to freeze-dry overnight. Important note: the glass flasks and Eppendorf tubes were weighed before filling in and after drying, which enabled the quantification of PCL (mg/ml) and enzyme SOD (mg/ml).

3.3.3 Dynamic light scattering

Dynamic light scattering (DLS) was performed to verify the hydrodynamic diameter of the nanoformulations and see their stability by polydispersity index values and continuous measurements over time. DLS is, in fact, one of the most common measurement techniques for particle size analysis in the nanometer range.

The DLS technique is based on the Brownian motion of dispersed particles. When particles are dispersed in a liquid, they move randomly in all directions[58]. The principle of Brownian motion is that particles are constantly colliding with solvent molecules, these collisions cause a certain amount of energy to be transferred, which induces particle movement. The energy transfer is almost constant and therefore has a greater effect on smaller particles[58]. As a result, smaller particles are moving at higher speeds than larger particles. If we know all the other parameters which influence particle movement, we can determine the hydrodynamic diameter by measuring the speed of the particles[58].

The relation between the speed of the particles and the particle size is given by the Stokes-Einstein equation

$$D = \frac{KbT}{6\pi\eta Rh} \quad \text{(Eq 3)}$$

The speed of the particle is given by the translational diffusion coefficient D, further, the equation includes the viscosity of the solvent (ŋ) and the temperature (T) because both parameters directly influence the particle movement[58]. A basic requirement for the Stokes-Einstein equation is that the movement of the particles needs to be solely based on Brownian motion.

The polydispersity index (PDI) is given to describe the broadness of the particle size distribution. A value below 10% reflects a monodisperse sample and indicates that all of the measured particles have almost the same size[58].

The assay was performed in a plastic cuvette, by adding 1ml of the solution of nanoformulations, and the hydrodynamic diameter was measured in the Delsa Nano submicron Particle size and Zeta potential.

3.4 Cellular assays

3.4.1 Cell culture assay

The cell linage used in the present study was HeLa cells. HeLa cells are the first immortal human cell line. The cell line grew from a sample of cervical cancer cells taken from an African-American woman named Henrietta Lacks on February 8, 1951. In 1953, Theodore Puck and Philip Marcus cloned HeLa cells for the first time. The cells were incubated in T25-flasks in the presence of *Dulbecco's Modified Eagle Medium* (DMEM) with 10% of fetal bovine serum (FBS), in an incubator at 37ºC with 5% of CO_2.

3.4.2 Flow cytometry

Flow cytometry is used to measure the physical characteristics of single particles, usually cells, as they flow in a fluid stream through a beam of light. The properties measured include a particle's relative size, relative granularity, and relative fluorescence intensity. These properties are determined using and optical-to-electronic coupling system that records how the cells scatter incident laser light and emit fluorescence[59].

A flow cytometer is composed of a flow chamber, which design causes the sample core to be focused in the center of the sheath fluid where the laser beam will then interact with the particles[59]. The flow cytometer is made up of three main systems: fluidics; the system that transports the cells in a stream to the laser beam for interrogation zone. It is divided into two types of fluids: the sheath fluid and the sample fluid, which cannot mix. The fluids are in parallel and the sample fluid pressure is always greater than the sheath fluid pressure [59].

The optical system; this system is composed of lasers to illuminate the particles in a sample fluid and by optical filters to direct the resulting light signals into electronic signals that can be processed digitally[59]. When particles pass through the laser, they scatter laser light into two types of scattering: forward scattering and side scattering. When the light is scattered and fluorescence emitted, these signals can reach appropriate detectors that will produce electronic signals, proportional to the optical signals[59]. The scattering of light occurs when a particle deflects incident laser light. The extent to which this occurs depends on the physical properties of a particle, namely its size and internal complexity. Factors that affect light scattering are the cell's membrane, nucleus, and any granular material inside the cell. Forward-scattered light (FSC) is proportional to the cell-surface area or size. The FSC is a measurement of mostly diffracted light and is detected just off the axis of the incident laser beam in the forward direction by a photodiode. It provides a suitable method of detecting particles greater than a given size independent of their fluorescence. The Side-scattered light (SSC) is proportional to cell granularity or internal complexity. It is a measurement of mostly refracted and reflected light that occurs at any interface within the cell where there is a change in the refractive index. The SSC is collected at approximately 90 degrees to the

laser beam by a collection lens and then redirected by a beam splitter to the appropriate detector[59].

The optical filters are responsible for the transmission of the light of a specific wavelength while reflecting other wavelengths. And the electronic system, which is responsible for light detection. The light detection is composed of photomultipliers (PTMs), which simply detect photons. The light needs to be optically filtered before, and then the photon energy is converted into a signal that is dependent on the number of photons and the voltage applied to the PTM. Photons are filtered, collected, and multiplied by the PTM, the current generated is converted to a voltage pulse, that will be digitized, and the values are stored into a List Mode File. Signals can be amplified by applying a voltage to the PMTs, thus creating a greater electrical current, or by increasing the amplification gain[59].

In the present study, flow cytometry was performed to verify the relative fluorescence intensity in HeLa cells, after being treated with fluorescent dyes, for both enzymes: SOD and ALP. The samples need to be prepared before performing the assay, by removing the medium and washing the cells with PBS. After washing the cells, it was required the addition of trypsin to generate a cell suspension. Then, it was added three times the amount of trypsin of DMEM without phenol red and the samples were collected into Eppendorf tubes, to be centrifugated. The samples were centrifugated at 1.2 rpm for 5 minutes. After centrifugation, it was necessary to remove the supernatant and add 200 µl of PBS.

The results were acquired in Gallios Flow cytometer 9 colors, 3 lasers from Beckman Coulter Life Sciences. By FlowingSoftware 2.5.1, the relative fluorescence intensity was measured. All fluorescent channels were used (FL1 to FL10), with the main focus on green channel (in case of SOD enzyme) and on the red channel (in case of ALP enzyme and nanoparticles that encapsulate rhodamine dye).

3.4.3 Fluorescence microscopy

Fluorescence microscopy is a method whereby fluorescent substances are examined in a microscope. The substance to be analyzed is excited with light of a shorter wavelength, usually blue or ultraviolet (UV), and then it is examined through a

filter that absorbs the short-wavelength light and transmits the fluorescence, which has a longer wavelength. This microscopy technique is useful for a range of advantages: great sensitivity for detection and quantification of small amounts of fluorescent substances or small particles, the possibility of application to opaque objects.

In the present thesis, the acquisition of fluorescence images of HeLa cells, after the treatment with nanoformulations: PCL and PCLALP, it was performed in the ZEISS microscope (ZEISS Axiovert 200M Fluorescence/Live cell imaging) with the ZEISS lite software (ZEN 3.1 Lite blue edition), to verify the uptake of nanoformulations by HeLa cells and the intensity of the fluorescent dye. The exposure time was 41.2 ms and it was used the channel HF594 (red channel) with a bandgap between 570-590nm.

Chapter 4

4 RESULTS AND DISCUSSION

4.1 Enzymatic assays

4.1.1 Quantification of protein concentration BCA-Protein assay

In Table 2 it is shown all the nanoformulations and their variations (with rhodamine dye, and with zinc and magnesium ions) PCL NP, PCLALP, and PCLSOD. All the concentrations are represented in units of mg/ml for PCLSOD nanoparticles and µg/ml for PCLALP nanoparticles.

Table 2 – PCL NPs with SOD and ALP (at different concentrations) with and without 0.1 mM of zinc and 1 mM of magnesium ions, and with 100 µl of rhodamine red dye. The numbers represent the concentrations of the encapsulated enzymes in mg/ml (SOD enzyme), and µg/ml (ALP enzyme), and in the case of rhodamine PCL NPs, it represents the amount of red dye encapsulated, in µl (Sigma Aldrich).

PCLSOD	**PCLALP**
PCLSOD0.02	PCLALP0.98
PCLSOD0.04	PCLALP0.98$zn_{0.1}mg_1$
PCLSOD0.05	PCLALP9.86
PCLSOD0.1	PCLALP9.86 $zn_{0.1}mg_1$
PCLSOD0.2	PCLRhod100
PCLSOD0.4	PCLALP0.98Rhod100

PCLSOD0.5	
PCLSOD1	
PCLRhod100	
PCLSOD0.1Rhod100	

It was important to formulate the nanoformulations with different amounts of enzymes to see which concentration or concentrations were more effective and to see in which enzyme concentration value, it is reached the saturation zone. In the case of PCLALP nanoformulations was important to verify not only the enzyme concentration but also the presence or absence of zinc and magnesium ions for enzymatic activity. Both ions are extremely important for ALP activity[53].

To proceed to the characterization of the nanoformulations created, which are PCL polymeric NPs encapsulating the enzymes SOD or ALP at different concentrations, it was performed the assay of BCA-Protein assay, as described in section 3.2.1. Through BCA-protein assay, it was possible to verify the concentrations of the enzymes encapsulated or adhered to the surface of the polymeric nanoparticle.

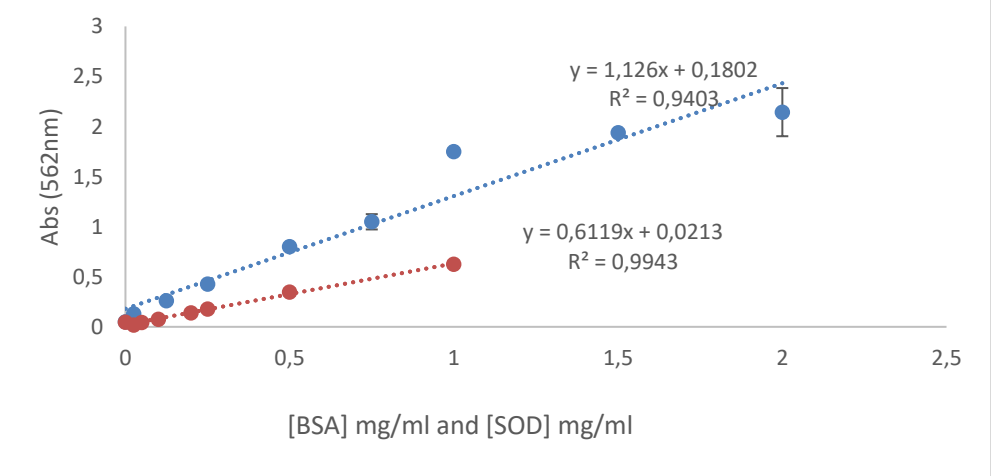

Figure 4 - BSA (blue dots) and SOD (red dots) calibration curves obtained by BCA-Protein Assay,

at 562 nm. Incubation at 37ºC for 30 min. Results were obtained using microplate reader Biotek synergy h1.

Table 3 – Concentration (mg/ml) of SOD encapsulated in PCLSOD nanoparticles (PCLSOD0.04 and PCLSOD0.2), by BCA protein assay.

Samples	**[SOD] mg/ml by BSA curve**	**[SOD] mg/ml by SOD curve**
PCLSOD0.2	0.013	0.290
PCLSOD0.04	0.018	0.030

By the results presented in Table 3, it is possible to verify that the calibration curve represented by SOD enzyme is more suitable than BSA calibration curve because it is showing experimental values (the ones that were obtained during the measurement), 0.290 mg/ml for PCLSOD0.2 and 0.030 mg/ml for PCLSOD0.04, are more close to the values of SOD concentration that was added for the synthesis of the nanoformulations (0.2 mg/ml of SOD in PCLSOD0.2, and 0.04 mg/ml of SOD in PCLSOD0.04).

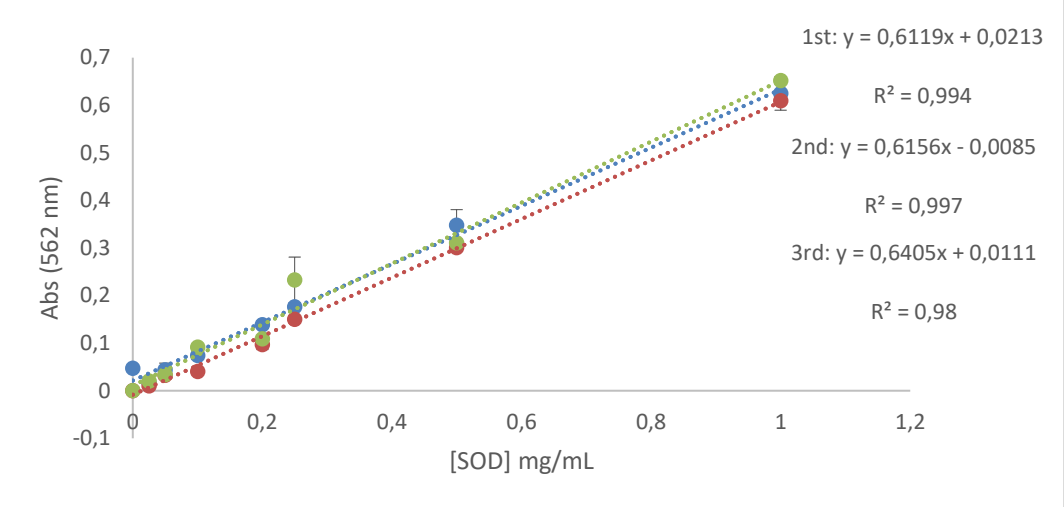

Figure 5 - SOD 1st calibration curve (blue dots); SOD 2nd calibration curve (red dots) and SOD 3rd calibration curve (green dots), obtained by BCA-Protein Assay, at 562 nm. Incubation at 37ºC for 30 min. Results were obtained using microplate reader Biotek synergy h1.

Table 4 - Concentration (mg/ml) values of superoxide dismutase in PCL NPs for all of the nanoformulations with the SOD enzyme.

Samples	**$[SOD]_{in\ PCL}$ mg/ml**
1st PCLSOD0.02	0.025
2nd PCLSOD0.02	0.029
1st PCLSOD0.04	0.030
2nd PCLSOD0.04	0.015
1st PCLSOD0.1	0.430
2nd PCLSOD0.1	0.420
1st PCLSOD0.2	0.290

1st PCLSOD0.5	0.320

As it is possible to verify in Table 4 the values that were obtained during the experiment are in general related to the ones that were added during the nanoprecipitation step, for the case of nanoformulations 1st and 2nd PCLSOD0.02; 1st PCLSOD0.04 and 1st PCLSOD0.2. But it is still required to perform an additional step which is more specific to know the concentration of the SOD enzyme encapsulated into PCL NPs. This step was accomplished by phase extraction and lyophilization step.

4.1.2 Intracellular Hydrogen Peroxide detection assay

The assay of intracellular hydrogen peroxide detection was performed to test if the enzyme SOD could maintain its activity after being encapsulated into PCL NPs and after being delivered into HeLa cells, by the endocytosis mechanism. As it was described in the state of the art section, 2.4.2 section, SOD is responsible for the dismutation of superoxide anion into hydrogen peroxide, so if it is verified that the cells are producing hydrogen peroxide, SOD enzyme is capable of maintaining its activity after being delivered.

The assay involved the addition of LPS at a concentration of 30 µg/ml, with an incubation time of 24h at 37ºC. The concentration of LPS added during the H_2O_2 detection assay was selected based on an additionally performed assay the LPS calibration curve. This assay was performed with an arrangement of LPS concentrations between 0-70µg/ml. In general, all the concentrations gave a good signal to the detection of intracellular H_2O_2. The concentration of 30µg/ml was the selected one since it is one of the lower amounts with a high fluorescent intensity signal. The LPS calibration curve is represented in the appendix section.

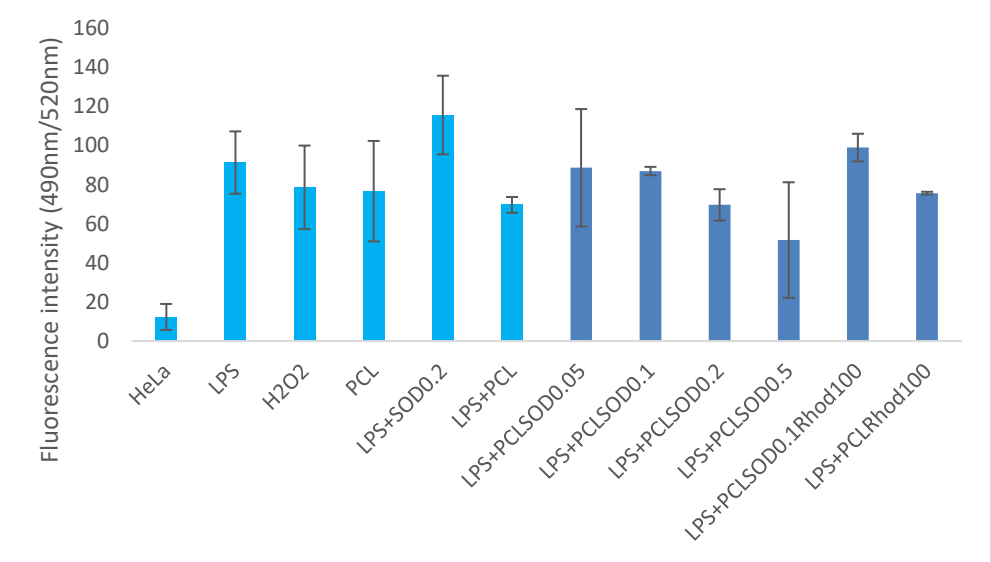

Figure 6 – Intracellular hydrogen peroxide detection assay by 1st batch of nanoformulations PCLSOD with different concentrations of SOD 0.05, 0.1, 0.2, 0.5, and PCL NPs with rhodamine encapsulated. In all the test samples, the HeLa cells were subjected to 30 µg/ml of LPS, and are represented by the dark blue bars. The control samples are represented by the light blue bars: 75000 cells/well HeLa cells, 30µg/ml LPS; 5mM H2O2; 30µg/ml LPS with 0.2mg/ml of SOD; PCL and 30µg/ml LPS with PCL. The incubation time of 4 h at 37ºC. The assay was performed in quadruplicates. Results were obtained using microplate reader Biotek synergy h1.

The HeLa cells were first added in a concentration of 75000 cells/well into the 48-well microplate in the day before the reading of the assay. As it is shown in Figure 6 the 75000 of HeLa cells in the medium, one of the control samples did not present a fluorescence signal after adding the green fluorescent dye into the well. This result shows that the cells were not generating by themselves intracellular H_2O_2. In terms of the other controls, HeLa cells subjected to 30 µg/ml of LPS and HeLa cells subjected to 5mM of H_2O_2, it is possible to verify that the HeLa cells after being subjected to them, responded with a high fluorescence intensity signal. This is according to the literature since LPS, even in a small amount (6 µg/ml), can increase the fluorescence intensity signal of hydrogen peroxide detection in HeLa cells, at the same incubation time, up to 50%[60]. In this present study, the signal increased up to 79% when compared to the control HeLa cells in DMEM.

One important result which is demonstrated in Figure 6 is the signal that is generated by adding PCL NP into the HeLa cells. So, why is PCL NP generating a signal that comes from the presence of intracellular hydrogen peroxide if this well was not subjected to the stimuli of LPS? And it is possible to answer this question in two ways: i) PCL NP is capable of leading to the production of H_2O_2 when enters in the cell through endocytosis mechanism, maybe because it generates some cell stress. Or ii) the nanoformulations are contaminated by some bacteria, and that contamination leads to the formation of hydrogen peroxide.

In terms of possibility i), the literature does not show, until now, studies about PCL inducing oxidative stress or production of hydrogen peroxide when entering in HeLa cells, only if the cells are already stimulated by another compound. But some cell lineages can suffer from transitory oxidative stress, after polycaprolactone enters by endocytosis mechanism, as L929 fibroblast[61]. It could be interesting for future work to study the potential oxidative stress of the PCL-derivative that was used in this thesis on HeLa cells.

To verify this hypothesis, it is important to test the possibility ii), which is said that the nanoformulations could have been contaminated by bacteria, this may happen during polymer synthesis or nanoparticle synthesis. In fact, during nanoprecipitation, as it is done with organic solvents, they can accumulate some residues that can be contamination that will degrade the encapsulated enzyme[56], or even during the test and due to long storage time. To verify this hypothesis, the different PCL and PCLSOD nanoformulations were incubated in LB-Agar, a bacteria growth medium. And they showed contamination, after 4 days of incubation, at room temperature.

To obtain clear results, it was performed a new step of nanoprecipitation with two different concentrations of SOD enzyme and PCL with rhodamine dye: PCL; PCLSOD0.1; PCLSOD0.5 and PCLSOD0.1Rhod100. This time, all the solutions and solvents (besides acetone) were filtered before adding and all the nanoprecipitation was done in the laminar airflow cabinet, the dialysis was done also in the laminar airflow cabinet, against autoclaved distilled water.

In Figure 6 it is possible to verify that the test samples could not increase the production of intracellular hydrogen peroxide not as much as the control sample

30µg/ml LPS. For example, the sample PCLSOD0.05 showed a decrease of hydrogen peroxide production, in comparison to the control one HeLa cells subjected to 30µg/ml LPS, of about 3%; the sample PCLSOD0.1 showed a decrease of about 5% comparing to the control HeLa cells subjected to 30µg/ml LPS; the sample PCLSOD0.2 showed a decrease of about 27% and the sample PCLSOD0.5 showed a decrease of about 50%. But, in terms of PCLSOD0.1Rhod100, it presented an increase of fluorescent intensity signal in comparison to the blank HeLa cells subjected to 30µg/ml LPS, of about 9%.

This result might be related to the less storage time (1 week at 4ºC), it was the last sample to be formulated in 1 week before performing this last assay. Either way, all the results are subjected to a close evaluation due to the bacteria contamination, because one question arises: the production of H_2O_2 is due to the presence of bacteria or due to the action of the encapsulated enzyme?

Another question that is important to answer is: which is more effective free 0.2mg/ml SOD or SOD encapsulated in PCL NPs? By Figure 6 it is possible to see an increase of fluorescence intensity signal of about 31% in the cells treated with 30µg/ml LPS plus 0.2mg/ml SOD when comparing to the blank HeLa cells treated with 30µg/ml LPS. In literature, it is said that the “Exo enzymes” that are administrated during enzyme replacement therapy face measuring obstacles due to low absorption and maintenance of structure and activity after their uptake by cells[1]. So, this result can be most justified by the presence of LPS, or by the fact that the green fluorescent dye has the weight enough to go in and out from the cell.

After performing another hydrogen peroxide detection step with the already non-contaminated nanoformulations, it is possible to get clear results. Another step that could be performed to verify the results is to verify by fluorescence microscopy if the dye is in the cells or not.

It was also tested another assay kit, the DCFDA ROS detection kit assay (supplied by Abcam chemicals), which operates in a close similar way to the one above. This kit uses the compound DCFDA (2´,7´-dichlorofluorescein diacetate) that after entering the cell is converted into a non-fluorescent compound deacetylated by cell esterases. If H_2O_2 is being generated in the cells, DCFDA is oxidized into DCF (2´,7´-

dichlorofluorescein) which has an excitation/emission wavelength of ex/em 485nm/535 nm.

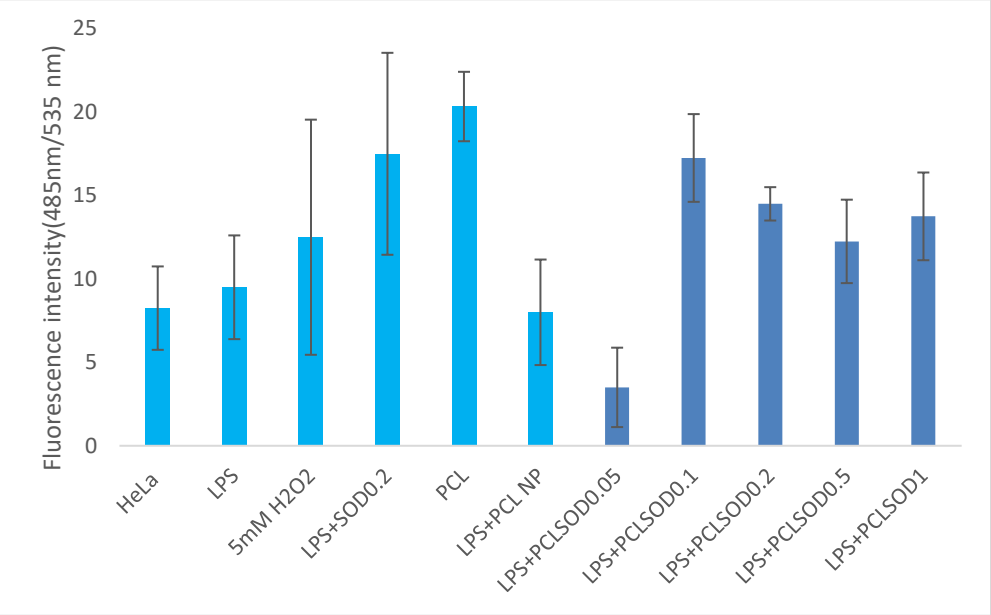

Figure 7 – DCFDA ROS detection assay by 2nd batch of nanoformulations PCLSOD with different concentrations of SOD 0.05, 0.1, 0.2, 0.5, and 1 mg/ml. In all the test samples, the HeLa cells were subjected to 30 µg/ml of LPS, and are represented by the dark blue bars. The control samples are represented by the light blue bars: 75000 cells/well HeLa cells, 30µg/ml LPS; 5mM H2O2; 30µg/ml LPS with 0.2mg/ml of SOD; PCL and 30µg/ml LPS with PCL. The cells were incubated for 4 h at 37ºC. The assay was performed in quadruplicates. Results were obtained using microplate reader Biotek synergy h1.

As in a similar way to the first tested kit, the DCFDA ROS detection assay showed an increase in fluorescence intensity signal after the 75000 cells/well HeLa cells were subjected to the PCL NP. This test sample showed an increase in fluorescence intensity signal when compared to the control sample 30µg/ml of LPS in HeLa cells.

In Figure 7 it is possible to verify that most of the test samples could increase the production of intracellular hydrogen peroxide even higher than the control sample 30µg/ml LPS. For example, the sample PCLSOD0.1 showed an increase of about 82%; the sample PCLSOD0.2 showed an increase of about 53%; the sample PCLSOD0.5 showed an increase of about 29% and the sample PCLSOD1 showed an increase of

about 45%. Either way, all the results are subjected to a close evaluation due to the bacteria contamination, as the ones got from the first kit assay.

4.1.3 Cellular viability assay using MTS reagent

The cellular viability assay was performed based on the reduction of the reagent MTS tetrazolium by viable mammalian cells that will generate a colored formazan dye that is soluble in cell culture media. This conversion is thought to be carried out by NADPH-dependent dehydrogenase enzymes in metabolically active cells. The product strongly absorbs at 496 nm.

The HeLa cells were subjected to a concentration of 125 µM H_2O_2. This concentration was selected based on literature[62], in which it is said that this concentration of hydrogen peroxide can promote apoptosis of HeLa cells by the mitochondria pathway, which leads to decontrolled oxidative stress of the cells. It inhibits cell growth of about 70%[62]. This apoptosis activation involves the upregulation of p73 and its downstream target Bax, which is responsible for the activation of the signal of cytochrome c release into the cytoplasm. After being released into the cytoplasm, cytochrome c activates a caspase signal cascade which is fundamental for the hydrolysis of cellular membrane proteins, which leads to cell death.

The HeLa cells were seeded and incubated overnight in a concentration of 15000 cells/well and 125 µM of H_2O_2 was added and incubated during 4 h, at 37ºC. After the action of hydrogen peroxide, it was administrated the control samples 15000 cells/well HeLa cells in DMEM; HeLa cells subjected to 125 µM H_2O_2; HeLa cells treated with 0.2mg/ml of SOD and HeLa cells treated with 50 µl of PCL NP into 100 µl of DMEM. And the test samples, the 2nd batch of nanoformulations PCLSOD, PCLSOD0.05, PCLSOD0.1, PCLSOD0.2, PCLSOD0.5, and PCLSOD1 with an incubation time of 4 h, at 37ºC. The enzyme SOD is known for its role in protecting cells against oxidative stress.

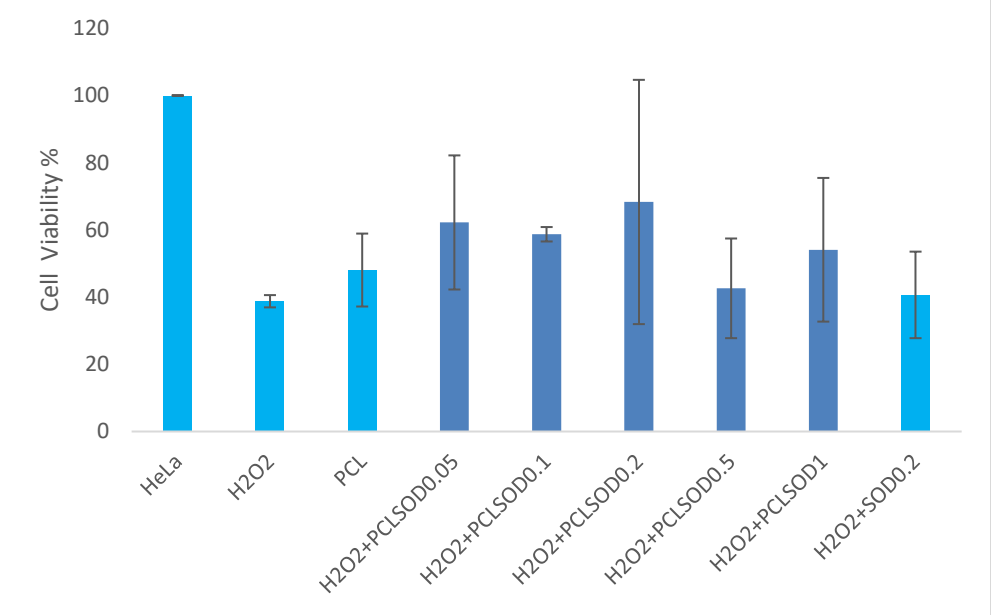

Figure 8 – HeLa cells viability assay carried out by MTS reagent. A concentration of 15000 cells/well was subjected to the nanoformulations PCLSOD with different concentrations of SOD 0.05, 0.1, 0.2, 0.5, and 1 mg/ml. The test samples represented by dark blue bars. In all the test samples, the HeLa cells were subjected to 125 µM of H_2O_2. The control samples are represented by the light blue bars: 15000 cells/well HeLa cells,125µM H2O2, 125µM with PCL NP, and 125µM with 0.2mg/ml of SOD. The cells were incubated for 4 h at 37ºC. The assay was performed in triplicates and the absorbance was read at 496nm. Results were obtained using microplate reader Biotek synergy h1.

As it is seen in Figure 8 the treatment of HeLa cells with 125 µM H_2O_2 reduced cell viability of about 40%. When the cells were treated with the nanoformulations this viability increased, for example, the nanoformulations PCLSOD0.05 and PCLSOD0.2 could increase the cell viability up to about 60%. The control sample HeLa cells that after the treatment with hydrogen peroxide were treated with 0.2mg/ml SOD enzyme, showed almost the same cell viability as the ones treated with only hydrogen peroxide. This can answer the question, does 0.2mg/ml of SOD is more effective than the enzyme encapsulated into PCL NPs? And In Figure 8 it is possible to verify that the SOD enzyme encapsulated in PCL NPs can protect cells against cell inhibition growth, caused by oxidative stress.

4.1.4 Alkaline phosphatase assay in solution: *p*-nitrophenyl phosphate assay

The compound p-nitrophenyl phosphate was used to test the activity of ALP in solution. Not only the activity was tested, but it was also important to verify if the temperature and the presence of zinc and magnesium ions influence the activity of ALP. The activity of ALP was tested free in solution and encapsulated in PCL NPs.

The assay was tested in two different temperatures 37 ºC and at 25 ºC for 60 minutes, both assays were performed in dark, to protect the yellow product p-nitrophenol. The results are represented in Figure 9, at 25 ºC, and in Figure 10, at 37 ºC.

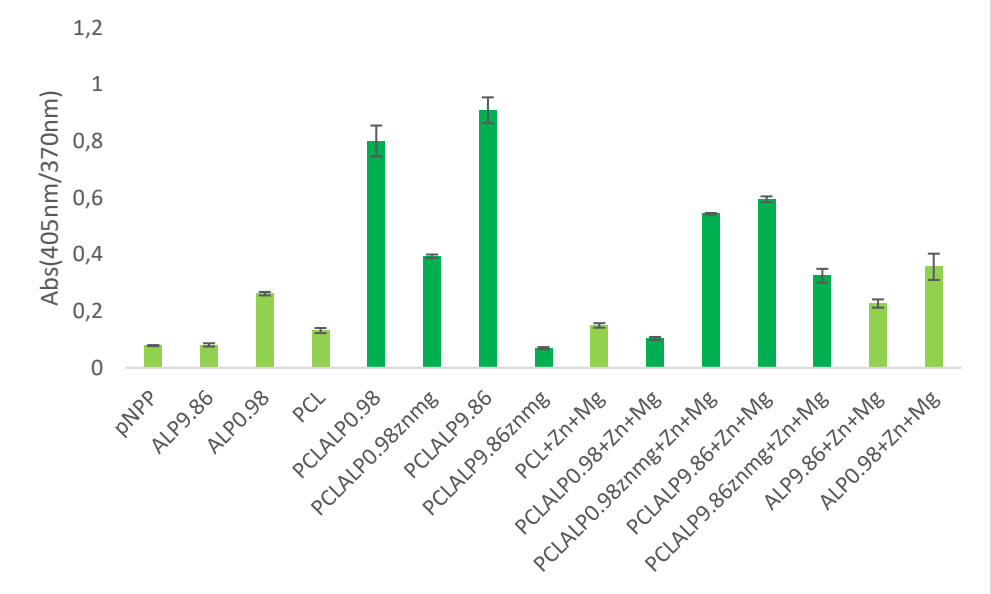

Figure 9 – Absorbance ratio between *p*-nitrophenol absorbance at 405 nm and *p*-nitrophenyl phosphate absorbance at 370 nm. All the samples were treated with 5mM of *p*NPP, mixed with 10 µl of ALP (free in solution and encapsulated in PCL NPs) in 40 µl of Tris-HCl 50mM pH 8.0, in a final well volume of 100 µl. The control samples are represented by light green bars and are divided between the ones without the addition of 0.1mM of Zn and 1mM of Mg, and with the addition of the metal ions. The test samples are represented by dark green bars and are divided between the ones without the addition of 0.1mM of Zn and 1mM of Mg, and with the addition of the metal ions. The experiment was carried at 25 ºC for 60 minutes and the absorbance was

read at 370nm and 405 nm in a microplate reader (Biotek synergy h1). The assay was performed in quadruplicates.

During this assay, the presence of $ZnCl_2$ and $MgCl_2$ metal ions was also tested to see their influence in substrate conversion. As it is possible to see in Figure 9 the test samples PCLALP0.98, PCLALP9.86 are the ones that show higher pNPP conversion (higher absorbance ratio), 0.80 and 0.91, respectively. The interesting thing in this result is the fact that both test samples were not synthesized in the presence of magnesium and zinc ions. The only difference between them is the amount of ALP that is encapsulated, 0.98 µg/ml, and 9.86 µg/ml. Both showed a higher conversion than the ones that were synthesized with magnesium and zinc ions. As it is possible to see, these samples also present a higher substrate conversion ratio than the control samples, 5mM of pNPP, ALP 9.86 µg/ml free in solution, ALP 0.98 µg/ml free in solution and 5mM pNPP with PCL NP. This result shows that the enzyme ALP has a higher action in PCL NPs than free in solution.

When it was added 0.1mM of ZnCl2 and 1mM of MgCl2 into the wells, it was verified that the test sample PCLALP0.98 lowered its capability of substrate conversion, since the ratio only reach the value of 0.10. This lowering on substrate conversion is due to the interference of metal ions concentration in ALP activity, which if they are not in their proper concentration, can inhibit enzyme activity[53]. The other test samples $PCLALP0.98_{zn0.1mg1}$ and $PCLALP9.86_{zn0.1mg1}$ showed an increase in their values of absorbance ratio 0.59, 0.54, respectively. It was possible to see the effect of zinc and magnesium ions when they are added into the wells, they have more effect than when they are added in the nanoprecipitation step.

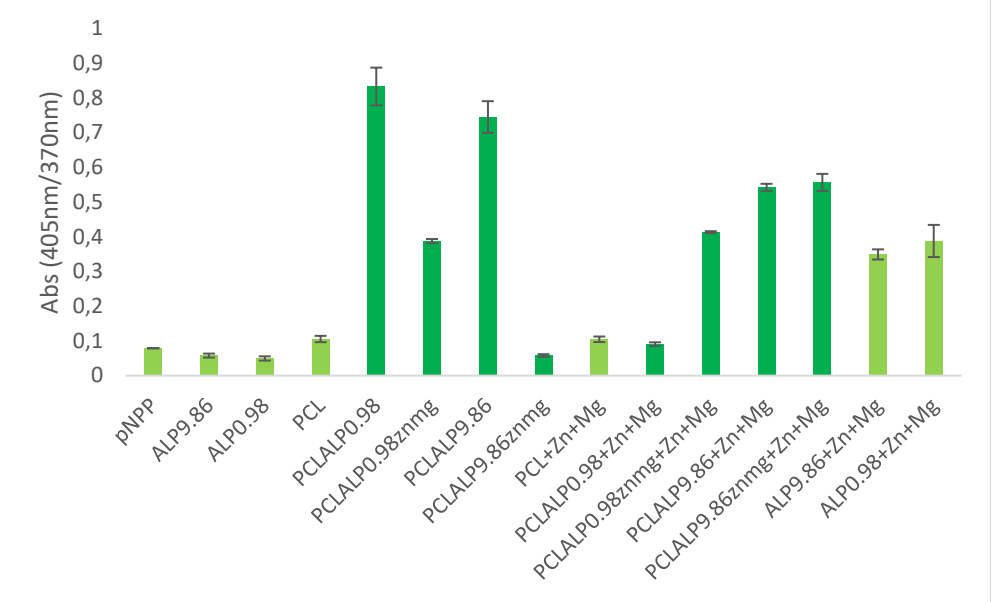

Figure 10 – Absorbance ratio between *p*-nitrophenol absorbance at 405 nm and *p*-nitrophenyl phosphate absorbance at 370 nm. All the samples were treated with 5mM of *p*NPP, mixed with 10 µl of ALP (free in solution and encapsulated in PCL NPs) in 40 µl of Tris-HCl 50mM pH 8.0, in a final well volume of 100 µl. The control samples are represented by light green bars and are divided between the ones without the addition of 0.1mM of Zn and 1mM of Mg, and with the addition of the metal ions. The test samples are represented by dark green bars and are divided between the ones without the addition of 0.1mM of Zn and 1mM of Mg, and with the addition of the metal ions. The experiment was carried at 37 ºC for 60 minutes and the absorbance was read at 370nm and 405 nm in a microplate reader (Biotek synergy h1). The assay was performed in quadruplicates.

The assay at 37 ºC is demonstrated in Figure 10 and the results are closely related to the ones that got it at 25 ºC. As it is possible to see, the nanoformulations PCLALP0.09, PCLALP9.06 are the ones that show higher pNPP conversion (higher absorbance ratio), 0.83, and 0.74, respectively. Again, the samples that were not synthesized in the presence of magnesium and zinc ions showed a higher conversion than the ones that were synthesized with magnesium and zinc ions. As it is possible to see, these samples also showed a higher substrate conversion ratio than the control samples, 5mM of pNPP, ALP 90.6 mg/ml free in solution, ALP 0.09 mg/ml free in solution and 5mM pNPP with PCL NP, which demonstrated that the enzyme ALP has a higher action in PCL NPs than free in solution.

When it was added 0.1mM of ZnCl2 and 1mM of MgCl2 into the wells, it was verified that the test sample PCLALP0.09 lowered its capability of substrate conversion, since the ratio only reach the value of 0.09. This lowering on substrate conversion is due to the interference of metal ions concentration in ALP activity, which if they are not in their proper concentration value, can inhibit enzyme activity[53]. The test sample $PCLALP9.06_{zn0.1mg1}$ demonstrated an increase in its absorbance conversion ration up to 0.56.

The most important remarks to take from para-nitrophenyl phosphate are the temperature does not have a strong influence in the enzyme-substrate conversion capability, since both assays showed similar results. The addition of metal ions has a stronger impact during microplate assay and not during the nanoprecipitation step. When it is increased the amount of ALP into PCL NPs the enzyme can lose some activity, but it can recover when it is added the proper amount of zinc and magnesium ions in solution. Finally, in general, the PCL NPs can confer some stabilization to the activity of ALP.

4.1.5 Alkaline phosphatase assay in cells: Naphthol AS-MX disodium salt assay

The activity of ALP in HeLa cells was verified by the red fluorescence substrate Naphthol AS-MX disodium salt. The assay was carried out in a 48-well microplate with incubations at 37 ºC. First, after seeding 75000 cells/well of HeLa cells, it was added the samples both tests and controls, during 4 hours at 37 ºC, and finally, it was applied 5 mM of the substrate for 45 minutes, at 37 ºC.

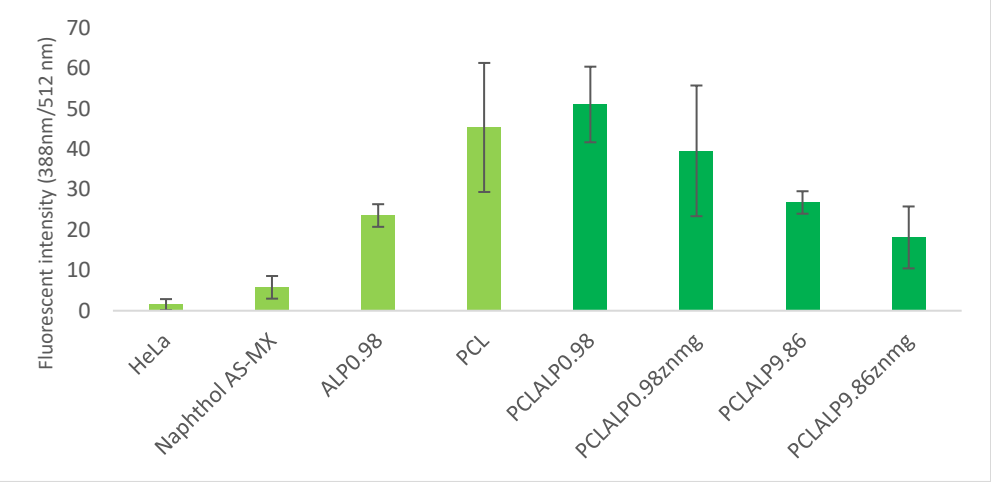

Figure 11 – Fluorescence intensity of Naphthol AS-MX disodium salt (ex/em=388/512nm). The assay was carried out with 5mM of Naphthol AS-MX disodium salt. The control samples are represented by light green bars, and the test samples are represented by dark green bars. The test samples are divided between the ones that are synthesized with 0.1mM of Zn and 1mM of Mg, and the ones that are synthesized without the addition of zinc and magnesium ions. The experiment was carried at 37 ºC for 45 minutes and the fluorescence intensity was read in the microplate reader BioTek synergy h1. The experiment was performed in quadruplicates.

There are important remarks to take it from Figure 11. As it is possible to verify, the control sample, 0.98 µg/ml of ALP free in DMEM with HeLa cells, showed that ALP free in solution, it is capable of hydrolyzing the substrate Naphthol AS-MX disodium salt since it reaches a fluorescence intensity value higher than the other control, 5mM of Naphthol AS-MX in HeLa cells. This result may be explained by the fact that some of the reaction can be occurring in solution, so, outside from the cell, because the ALP and most of the enzymes have some difficulty to cross by itself the cell membrane without compromising their activity and structure.

The test samples PCLALP0.98 and PCLALP0.98$_{zn0.1mg1}$ showed the highest fluorescence intensity among all samples. And if we compared to the control sample, only 5mM of Naphthol AS-MX disodium salt, it is possible to verify that encapsulated 0.98 µg/ml ALP can hydrolyze the substrate after being delivered into cells. And this action is responsible for the exogenous ALP and not the endogenous ones since the substrate by itself is not fluorescent, it is only fluorescent when it reacts with alkaline phosphatase. So, if the control sample, 5mM Naphthol AS-MX, presents a fluorescence

intensity value close to the control sample, 75000 cells/well of HeLa, it is possible to see that the endogenous enzymes could not interfere with the conversion of substrate into a fluorescent product, in this case.

These results were also tested by flow cytometry to be confirmed, and one important question remains: The reaction is occurring in the intracellular or extracellular medium? Does the signal come from inside of the cell? To answer these questions cell images were taken in a fluorescence microscope.

4.1.6 Flow cytometry

Flow cytometry technique was performed to enable the verification of the results obtained from the microplate reader. This technique not only gives the results of fluorescence intensity but also by side and forward scattering provides information about cell morphology. For flow cytometry and fluorescence microscopy assays were also used PCL NPs encapsulating the red fluorescent dye rhodamine. Rhodamine enabled us to verify if the nanoformulations were uptake or not.

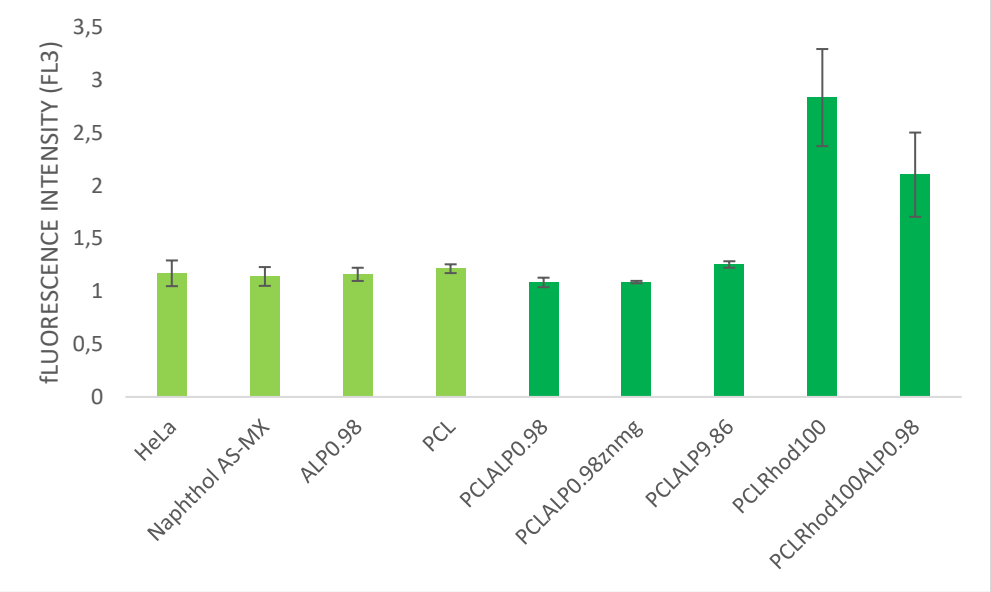

Figure 12 – Fluorescence intensity of Naphthol AS-MX disodium salt (ex/em=388/512nm). The

assay was carried out with 5mM of Naphthol AS-MX disodium salt. The control samples are represented by light green bars, and the test samples are represented by dark green bars. The test samples are divided between the ones that are synthesized with 0.1mM of Zn and 1mM of Mg, and the ones that are synthesized without the addition of zinc and magnesium ions. The experiment was carried at flow cytometer Gallios Flow cytometer 9 colors, 3 lasers from Beckman Coulter Life Sciences. The results were acquired in triplicates, using the FL3 (red) channel.

In Figure 12 it is demonstrated that there is no difference between control and test samples. When flow cytometry results are compared with the microplate results, it is possible to verify that the substrate 5mM naphthol AS-MX disodium salt is not being cleaved by endogenous ALP enzyme, since there is almost no difference between the untreated cells (75000 cells/well HeLa cells) and the cells treated with just 5mM of the substrate. The results got from flow cytometry are not following the ones got from microplate readers in terms of the action of PCLALP NPs. Figure 12 shows that the nanoformulations could not successfully deliver ALP to the HeLa cells without compromising its activity. For example, in the case of PCLALP0.98, in Figure 11, this nanoformulation reach a value of fluorescence intensity which is different and a little bit higher than the control one (5mM of Naphthol AS-MX in 75000 cells/well HeLa), and in Figure 12 reach a value which is closer or even lower than the control samples, 75000 cells/well HeLa, 5mM Naphthol AS-MX and 5mM Naphthol AS-MX with PCL NP. This makes us question if the reaction is occurring outside of the intracellular environment of the cells. To answer this hypothesis, it was performed a visualization of HeLa cells by fluorescence microscopy, as it is going to be discussed in the next section.

One interesting result present in Figure 12 is the fact that the nanoformulation PCLALP0.98Rhod100 was the only one that showed an increase in fluorescence intensity signal, even higher than the control samples, 75000 cells/well HeLa, 5mM Naphthol AS-MX and 5mM Naphthol AS-MX with PCL NP. This sample was not prepared at the same time as the others, so maybe the less store and refrigeration time could protect the stability of the activity of ALP. Or this value is justified by the presence of rhodamine dye, a red dye, which is the most likely hypothesis.

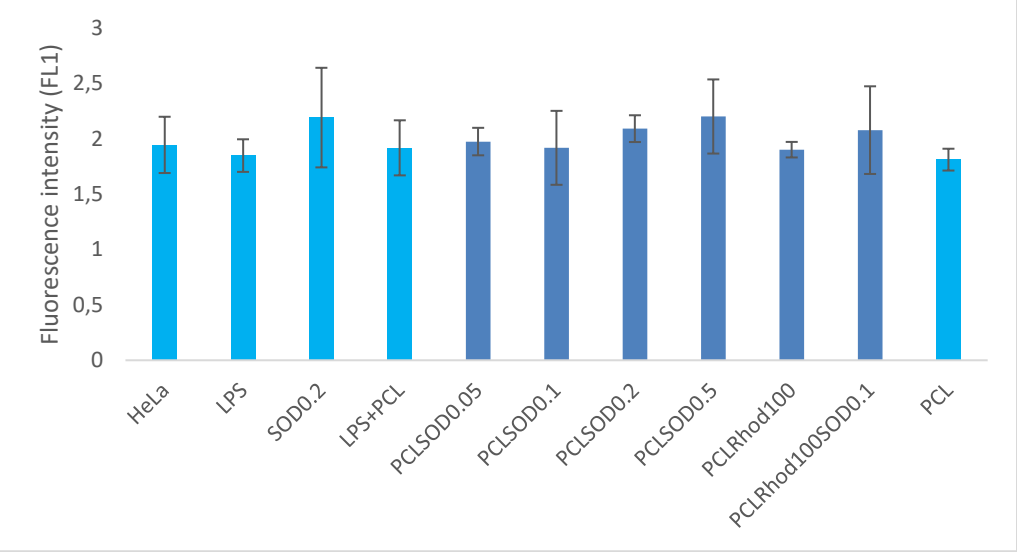

Figure 13 – Fluorescence intensity of intracellular detecting H_2O_2 green dye (ex/em=490nm/520nm). The 750000 cells/well of HeLa cells were treated with 30 µg/ml of LPS, both control, and test samples. The control samples are represented by light blue bars, and the test samples are represented by dark blue bars. The experiment was carried at flow cytometer Gallios Flow cytometer 9 colors, 3 lasers from Beckman Coulter Life Sciences. The results were acquired in triplicates, using the FL1 (green) channel.

From SOD enzyme flow cytometry results represented in Figure 13, it is not possible to see a clear difference between the untreated cells (75000 cells/well HeLa cells), the control samples, and the test samples. For example, the control sample 75000 cells/well HeLa presents a value of fluorescence intensity (1.95) which is close to the value of the test sample PCLSOD0.1 (1.92). By flow cytometry results it is possible to consider the hypothesis that the reaction is occurring in the extracellular environment. The green fluorescent dye is small enough to go in and out from the cell membrane, and if SOD is not being successfully delivered into cells, this might have happened. These results are important to be tested by fluorescence microscopy to verify the interior of the HeLa cells and see if it is possible to get the green signal from the intracellular dye. By flowing software 2.5 it was also analyzed the results got form channel FL3 (red channel), for the test samples: PCLRhod100 and PCLSOD0.1Rhod100.

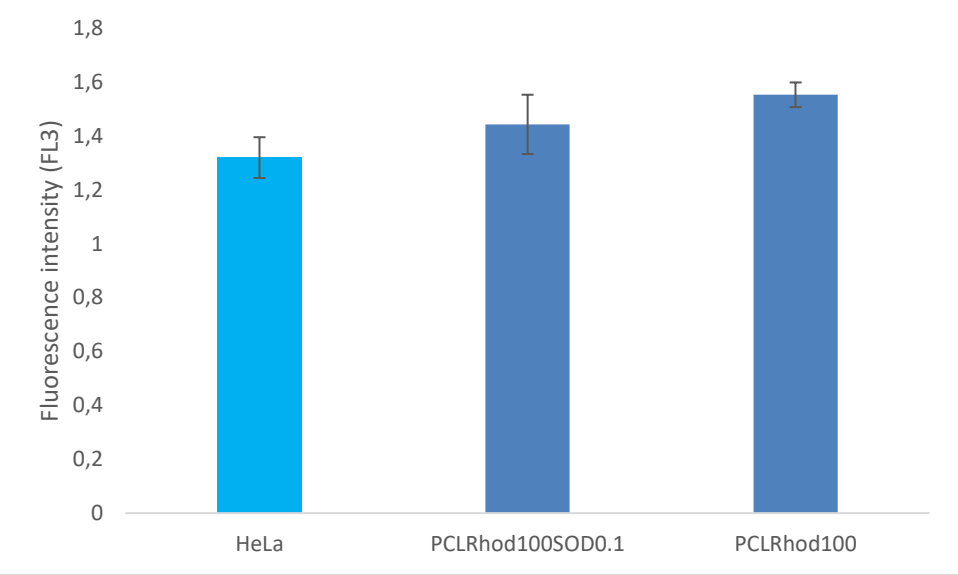

Figure 14 – Fluorescence intensity of rhodamine red dye-PCL nanoparticles used during intracellular detecting H_2O_2 green dye (ex/em=490nm/520nm) assay. The 750000 cells/well of HeLa cells were treated with 30 µg/ml of LPS, both control, and test samples. The control sample is represented by a light blue bar, and the test samples are represented by dark blue bars. The experiment was carried at flow cytometer Gallios Flow cytometer 9 colors, 3 lasers from Beckman Coulter Life Sciences. The results were acquired in triplicates, using the FL3 (red) channel.

In Figure 14 it is possible to verify that the nanoformulation PCLRhod100 was successfully delivered into cells, by presenting a fluorescence intensity value of about 1.55. The nanoformulation PCLSOD0.1Rhod100 presented a value of 1.44, in comparison to the value got for the untreated cells (just HeLa cells), 1.32. This result might mean that the nanoformulation was successfully delivered into HeLa cells, but the SOD activity was compromised by the endocytosis mechanism or during the nanoprecipitation step when encapsulating both rhodamine dye and SOD enzyme.

4.1.7 Fluorescence microscopy

The fluorescence microscopy analysis was performed to visualize the uptake of HeLa cells for the fluorescent dye Naphthol AS-MX phosphate (red dye) to test the uptake of ALP delivered by PCL NPs. This technique was also used to test the uptake

of rhodamine red dye by HeLa cells, and if possible, the localization within the cell. The activity or uptake of HeLa cells for the enzyme SOD was not able to be performed during the time of this thesis.

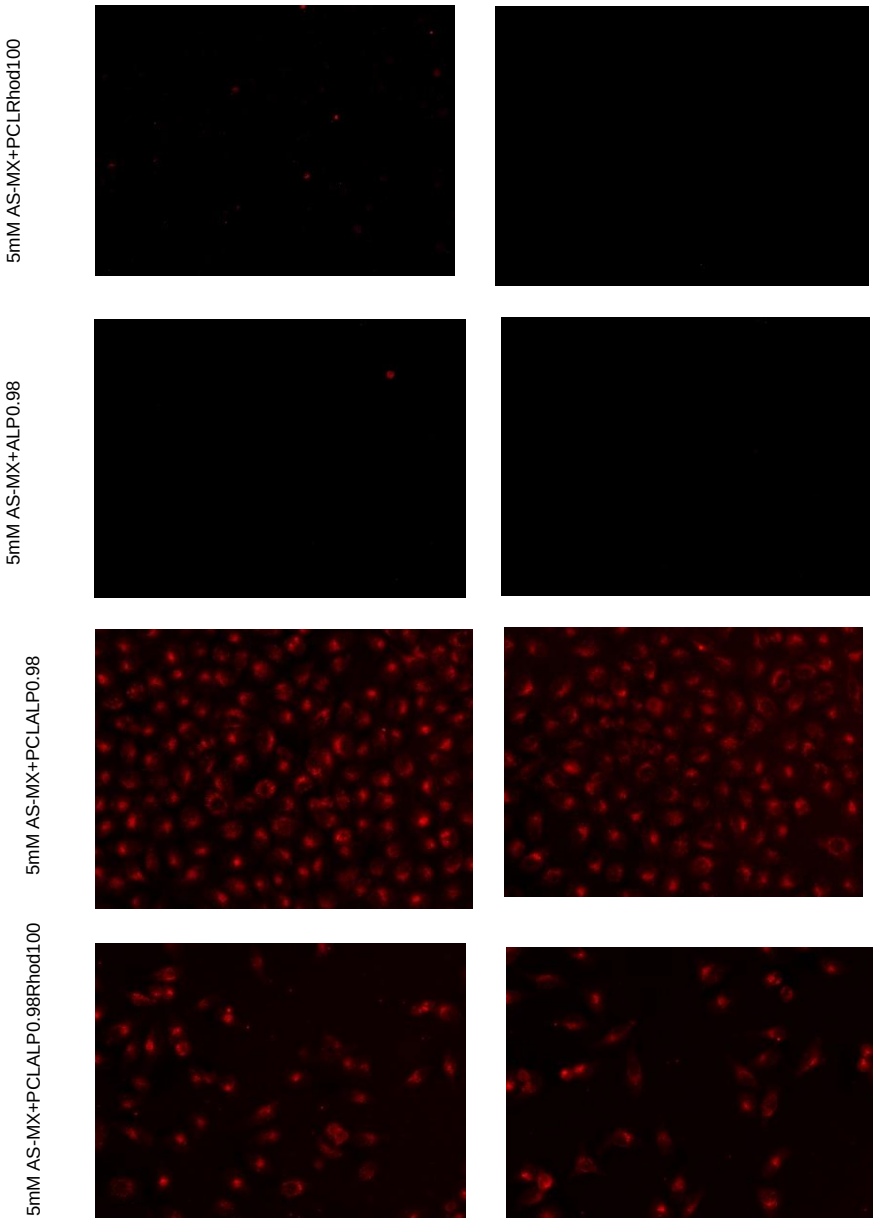

Figure 15 – Fluorescence microscopy images of HeLa cells after treatment with nanoformulations PCLALP0.98; PCLALP0.98Rhod100; PCLRhod100 and the control sample ALP0.98. Images were taken with ZEISS microscope (ZEISS Axiovert 200M Fluorescence/Live cell imaging), red channel HF594 with an exposure time of 41.2 ms, and a bandgap between 570-590nm. Images were analyzed with ZEN 3.1 life blue edition.

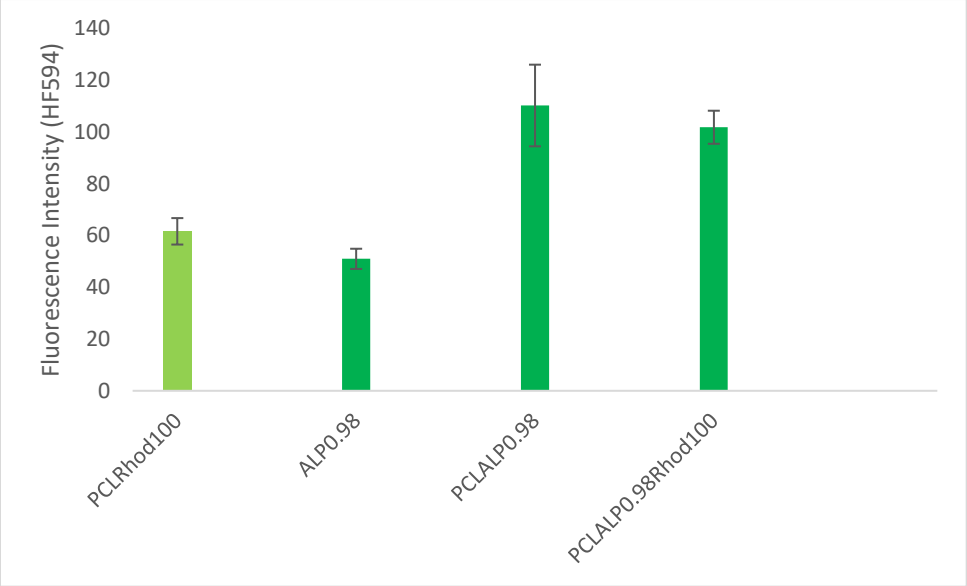

Figure 16 – Fluorescence intensity of HeLa cells after the treatment with PCLALP NPs. All the samples were subjected to 5mM of Naphthol AS-MX, and the assay was carried out with a concentration of 750000 cells/well of HeLa cells. The control sample is represented by a light green bar, and the test samples are represented by dark green bars. The results were analyzed with ZEEIS software, ZEN 3.1 life blue edition.

As it is demonstrated in Figure 15, the fluorescence images showed that the uptake of HeLa cells for the nanoformulations PCLALP0.98 and PCLALP0.98Rhod100 was successful. They are the ones that showed a higher fluorescence intensity value, as it is possible to see in Figure 16, 110.21, and 101.80, respectively. In comparison with the control sample ALP0.98, that has a fluorescence intensity value of 61.60.

The nanoformulation PCLRhod100 was not successfully delivered into HeLa cells, as it is possible to see in Figure 15, and in Figure 16 that only reaches a value

of 50.97. This can be explained by the fact that during the nanoprecipitation step, the rhodamine dye was not successfully encapsulated. It is important to remind that the fluorescence microscopy analysis of PCLALP NPs was carried out 1 week later after the flow cytometry assay.

4.2 Characterization of polymeric nanoparticles

4.2.1 Dynamic Light Scattering

The DLS technique was used to verify the hydrodynamic diameter of the nanoformulations synthesized, PCLALP, and PCLSOD nanoparticles. Besides the value of their hydrodynamic diameter (nm), it was verified the value of PDI to see the homogeneity of the samples.

In figures, 17A to 17E the values of hydrodynamic diameter of each sample measured during the time (1 day after precipitation; 1 week after precipitation and 1 month after precipitation) for PCLSOD nanoparticles, are represented. The measurement at different times after synthesis enables the verification of the stability of the nanoformulations.

A

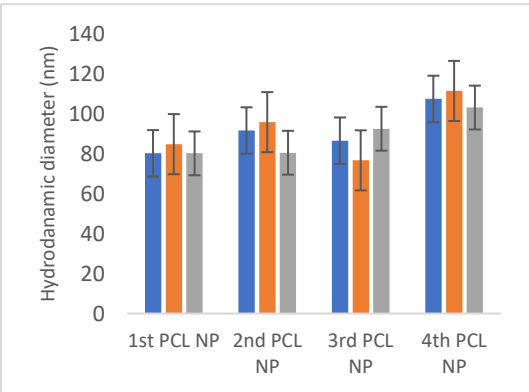

B

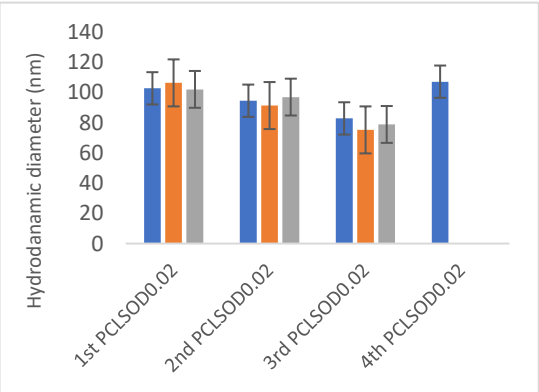

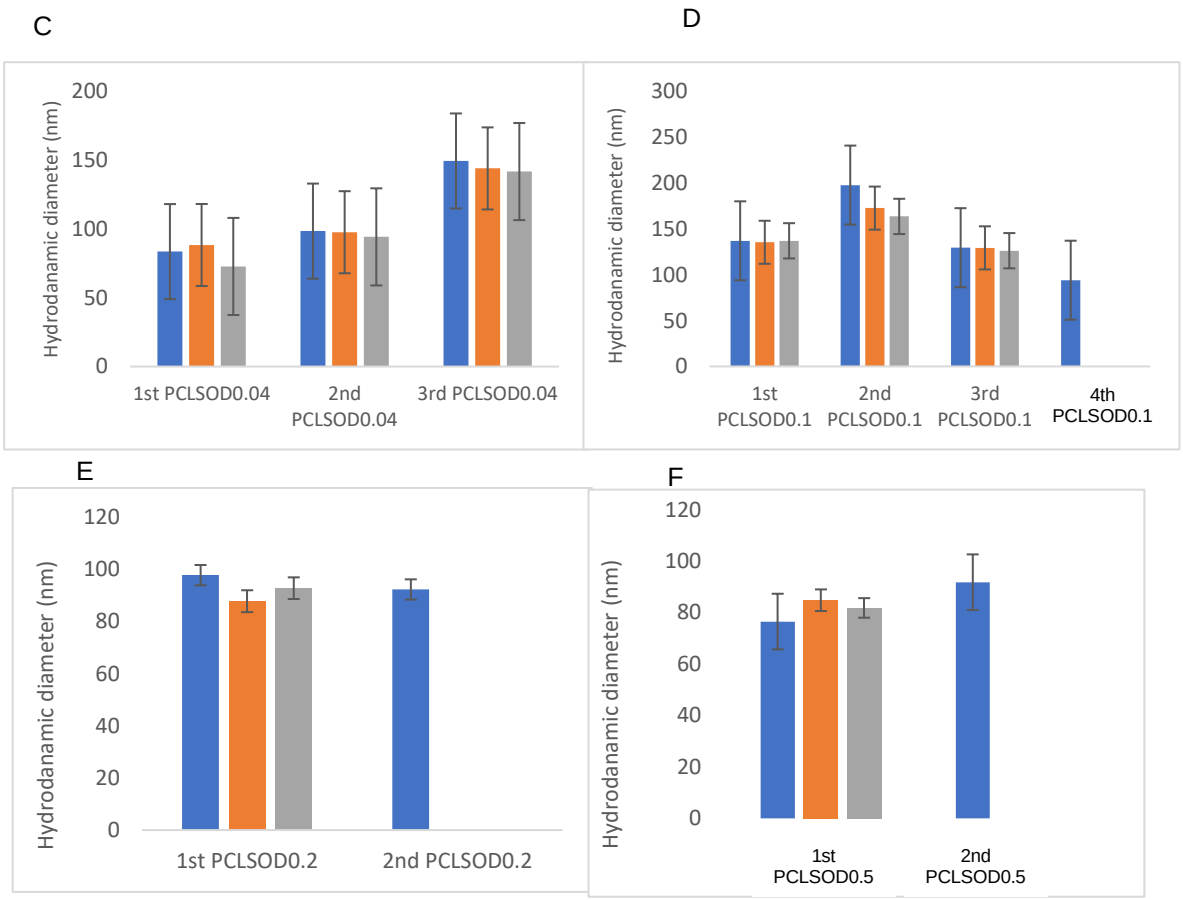

Figure 17 – Hydrodynamic diameter (nm) of nanoformulations PCLSOD measured by DLS in the DelsaNano C particle analyzer from Beckman Coulter. Figure 17A is represented the different batches of PCL NP synthesized. Figure 17B: PCLSOD0.02 NP. Figure 17C: PCLSOD0.04 NP. Figure 17D: PCLSOD0.1 NP. Figure 17E: PCLSOD0.2 NP. And figure 17F: PCLSOD0.5 NP. Blue bars: hydrodynamic diameter after 1 day of nanoprecipitation; orange bars: hydrodynamic diameter after 1 week of nanoprecipitation and grey bars: hydrodynamic diameter after 1 month of nanoprecipitation.

As it is possible to see in Figures 17A to 17F the nanoformulations PCL and PCLSOD maintained their hydrodynamic diameter mostly constant over time, presenting the same value with lower variation during all measurements.

Table 5- PDI average values for each PCLSOD NP obtained with DelsaNano C particle analyzer from Beckman Coulter

Sample	PDI
1st PCL NP	0.174±0.006
2nd PCL NP	0.162±0.008
3rd PCL NP	0.159±0.024
4th PCL NP	0.123±0.015
1st PCLSOD0.02	0.192±0.005
2nd PCLSOD0.02	0.127±0.007
3rd PCLSOD0.02	0.2±0.028
4th PCLSOD0.02	0.127
1st PCLSOD0.04	0.175±0.007
2nd PCLSOD0.04	0.154±0.015
3rd PCLSOD0.04	0.175±0.017
1st PCLSOD0.1	0.108±0.003
2nd PCLSOD0.1	0.12±0.015
3rd PCLSOD0.1	0.156±0.004
4th PCLSOD0.1	0.155

1st PCLSOD0.2	0.196±0.025
2nd PCLSOD0.2	0.1
1st PCLSOD0.5	0.136±0.024
2nd PCLSOD0.5	0.15

By PDI values it is possible to infer that the nanoformulations PCLSOD and PCL NPs are homogeneous, they are monodisperse nanoparticles.

In Figure 18 it is present the hydrodynamic diameters of the nanoformulations PCLALP. The values were taken 1 day after the nanoprecipitation step.

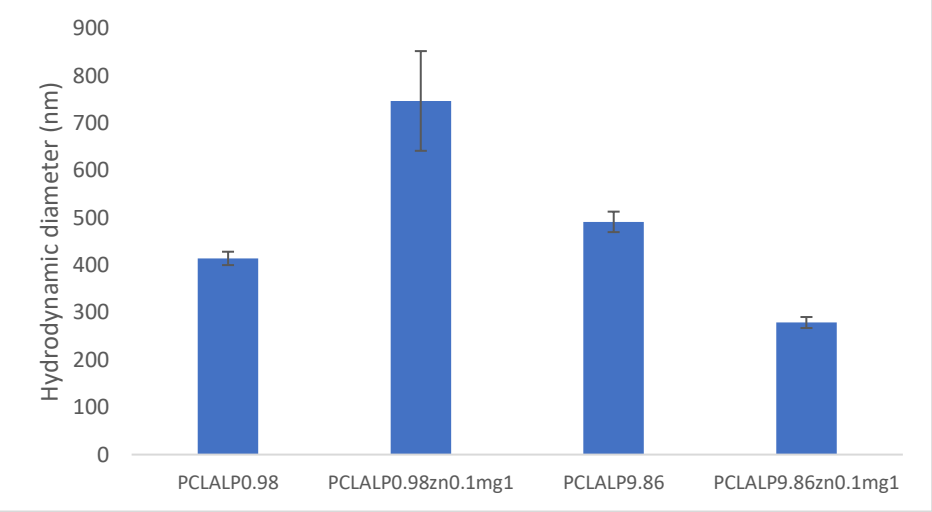

Figure 18 – Hydrodynamic diameter (nm) of nanoformulations PCLALP measured by DLS in the DelsaNano C particle analyzer from Beckman Coulter. Blue bars: hydrodynamic diameter after 1 day of nanoprecipitation.

By the values of the hydrodynamic diameter of PCLALP represented in Figure 18, it is possible to verify that the values are higher than the ones obtained for PCLSOD. For example, for PCLALP0.98$zn_{0.1}mg_1$ to reach a value of 746.56 nm, these values could be caused by the presence of the metal ions zinc and magnesium. Besides this factor

the size of the ALP enzyme is higher than of the SOD enzyme, 86 kDa compared to 32 kDa.

Table 6- PDI average values for each PCLALP nanoparticle obtained with DelsaNano C particle analyzer from Beckman Coulter.

Sample	PDI
PCLALP0.98	0.116
$PCLALP0.98_{zn0.1mg1}$	0.17
PCLALP9.86	0.107
$PCLALP9.86_{zn0.1mg1}$	0.129

By PDI values it is possible to infer that the nanoformulations PCLALP are homogeneous, presenting a value of PDI which is characteristic of monodisperse nanoparticles.

In Figure 19 it is present the hydrodynamic diameters of the nanoformulations PCLRhod100 and PCLALP0.98Rhod100. The values were taken 1 day after the nanoprecipitation step.

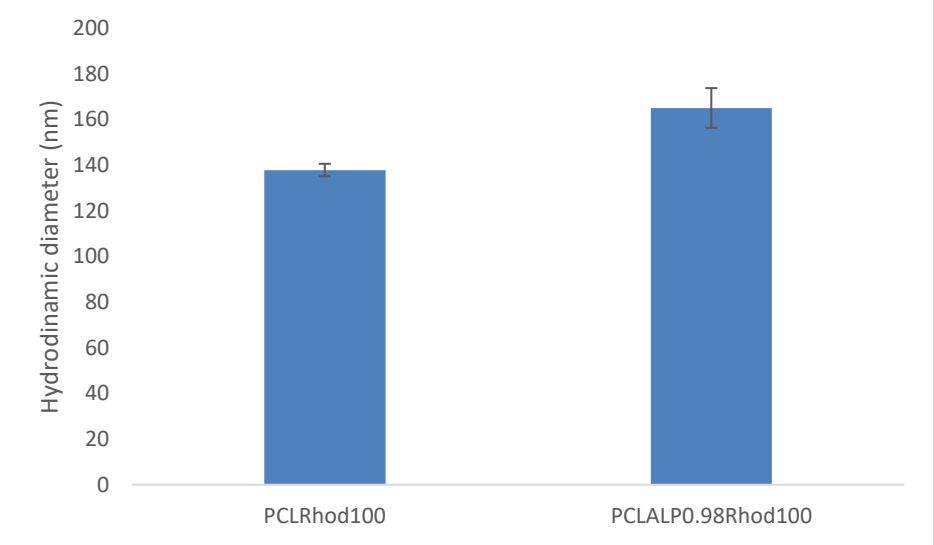

Figure 19 – Hydrodynamic diameter (nm) of nanoformulations PCLRhod100 and PCLALP0.98Rhod100, measured by DLS in DelsaNano C particle analyzer from Beckman Coulter. Blue bars: diameter after 1 day of nanoprecipitation.

By the values of hydrodynamic diameter of PCLRhod and PCLRhod with the ALP enzyme presented in Figure 19, it is possible to verify that the values maintained close to the ones got for the nanoformulations without the addition of rhodamine. For example, for the case of the ALP enzyme, the system PCLALP0.98Rhod100 presented a value of 165.1 nm and PCLALP0.98 presented a value of 400 nm. In this case, it can be verified that the enzyme or the red dye was not successfully encapsulated.

Table 7- PDI average values for each PCLRhod nanoparticle obtained with DelsaNano C particle analyzer from Beckman Coulter.

Sample	PDI
PCLRhod100	0.115
PCLALP0.98Rhod100	0.187

4.2.2 Phase extraction and Lyophilization

The phase extraction and lyophilization step were performed to characterize the nanoformulations PCL and PCLSOD to enable the calculation of the amount of enzyme encapsulated during the nanoprecipitation step. Two different organic solvents were used, dichloromethane and chloroform.

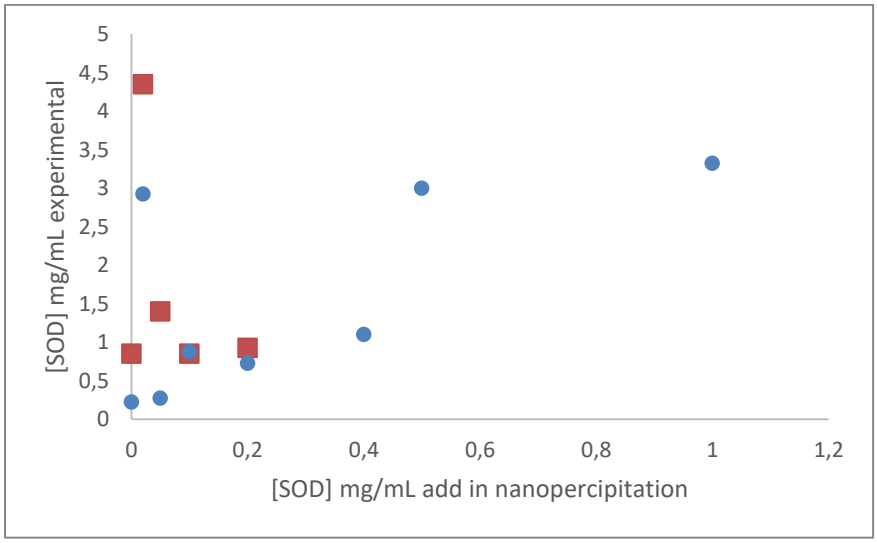

Figure 20 – Phase extraction and lyophilization of nanoformulations PCL and PCLSOD. Presenting the [SOD] mg/ml experimental values, the ones that are obtained after weighted the Eppendorf and small glass flasks, versus [SOD] mg/ml added in nanoprecipitation step. The blue dots series are the values obtained by using chloroform as the organic solvent, and the red squares are the values obtained by using dichloromethane as the organic solvent.

By Figure 20 it is possible to infer that the step of phase extraction was not successful accomplish since the experimental values of [SOD] mg/ml did not match the ones that were added. For example, when it was added 0.1 mg/ml during nanoprecipitation, it was got 1 mg/ml after the lyophilization step. Besides this factor, the values did not reach a stabilization, a saturation. Not with dichloromethane, but there is some signal with chloroform. The full characterization of the nanoformulations is one step that needs to be repeated and improved to fully properly characterized the nanoparticle systems.

Chapter 5

5 CONCLUSION

5.1 Superoxide dismutase approach

To conclude the study presented in this thesis of Polycaprolactone nanoparticles as carriers for delivery of enzymes into cells, in terms of SOD enzyme, it was possible to see, in Figure 6 (microplate assay for detection of intracellular H_2O_2 by the green detecting dye), all the cells without LPS or hydrogen peroxide subjection were in the absence of oxidative stress. HeLa cells without any stimuli did not present a fluorescence intensity signal of H_2O_2. The assay was performed with the first set of PCL NPs with the SOD enzyme, which was with bacteria contamination. All these nanoformulations could not increase the fluorescence intensity signal. The nanoformulation PCL NP gave a higher signal of fluorescence intensity, and this result may be explained due to bacteria contamination. In this set of particles, only the nanoformulation PCLSOD0.1Rhod100 could increase the signal, higher than the signal of control sample HeLa treated with 30 µg/ml of LPS. This may be explained by a lower incubation time (1 week at 4ºC), leading to the protection of the nanosystem's integrity.

The intracellular detection of hydrogen peroxide was performed again with the second set of particles and with another kit: DCFDA ROS detecting kit, which showed better results. In these assays, we could see a more clear difference between the control and test samples. In Figure 7, it is possible to verify that the nanoformulations PCLSOD0.1, PCLSOD0.2, PCLSOD0.5, and PCLSOD1 could increase more significantly the production of hydrogen peroxide than the control sample (HeLa cells treated with 30 µg/ml of LPS). But, in the end, we could not conclude if the free enzyme 0.2 mg/ml SOD could have been more effectively delivered into cells than SOD encapsulated into PCL NPs, and we still have a higher signal in the cells treated with PCL NP. The set of NPs contaminated with bacteria, made us doubt whether the reaction was occurring in the intracellular or extracellular environment. The results were not clarified by flow cytometry analysis and fluorescence microscopy.

In the MTS cell viability assay (Figure 8), it was possible to see that 0.2 mg/ml of free SOD was not able to protect the cells against cell inhibition growth. In general, all the other nanoformulations, the 2nd batch of PCLSOD, could increase the cell growth, protecting the cells from oxidative stress.

In the flow cytometry analysis, represented in Figures 13 and 14, it was not possible to see a clear difference between the control and test samples that were delivered into HeLa cells. This assay was performed with the second set of particles also, and with PCLSOD0.1Rhod100. This last NP was the one that could increase the signal of fluorescence intensity a little bit higher than the control sample (75000 cells/well HeLa, when using the red channel FL3, the red one). This result may indicate that the SOD enzyme could not be successfully delivered to the HeLa cells. This could be to either loss of activity in the encapsulation step or its activity being compromised by the bacteria contamination. But there is some signal in the red channel that comes from the encapsulation of rhodamine dye (Figure 14).

All these steps need, however, to be performed again with a new non-contaminated set of particles in order to obtain more conclusive results.

5.2 Alkaline phosphatase approach

To conclude the ALP approach that is presented in this research work, it was possible to see that in the *p*-nitrophenyl phosphate assay in solution (Figures 9 and 10), PCL NPs could protect the enzyme in solution. It could maintain its activity since the nanoformulations PCLALP0.98, 0.98 and 9.86 µg/ml ALP, respectively, gave a higher substrate (p-nitrophenol) conversion ratio than the free enzyme in solution.. The activity assay tested under two different temperatures, 25 ºC and 37 ºC, showed no relevant difference between these two temperatures. So, in this case, ALP activity did not depend strongly on temperature. The addition of the zinc and magnesium ions that are important for ALP activity has more impact when added during the assay, so in solution into the well, than when added during the nanoprecipitation step.

In the naphthol AS-MX disodium salt assay in HeLa cells, the nanoformulations PCLALP0.98 and PCLALP0.98$_{zn0.1mg1}$ were the ones that gave a higher fluorescence

signal, so the ones that could hydrolyze the substrate better. The interesting part of this result is the fact that the nanoformulation PCLALP0.98 was also the one that gave a higher substrate conversion ratio in the pNPP assay in solution. So, maybe 0.98 µg/ml ALP encapsulated in PCL NP is a concentration that is possible to be added without compromising enzyme activity after being delivered into cells. In Figure 11 is possible to see that the enzymes that are responsible to cleave the substrate are the ones that are being delivered and not the endogenous ALP enzymes. At the end of this assay, one question remains to be answered: what is more effective, free ALP, or ALP encapsulated into PCL NP? Since free 0.98 µg/ml of ALP could hydrolyze the substrate naphthol AS-MX with a result close to the PCLALP NPs, this result may also be explained by the fact that maybe this reaction is occurring in the extracellular environment.

The flow cytometry results that were presented in Figure 12 do not have the same meaning as in Figure 11 (microplate assay of naphthol AS-MX) since all tested samples did not show a difference to the control samples. But, we can answer the question that maybe this reaction is occurring in the extracellular environment so that naphthol AS-MX may not have been successfully delivered into HeLa cells. Or, ALP enzyme may have lost some of its activity after being transported into cells. The nanoparticle PCLALP0.98Rhod100 gave a higher fluorescence intensity signal than the other tested samples PCLALP. Still, as the substrate is also red, it is not possible to be sure if the signal that we are reading comes from the naphthol AS-MX conversion or from rhodamine dye.

In fluorescence microscopy results (Figures 15 and 16), it was possible to verify that the nanoformulation PCLALP0.98 was successfully delivered into HeLa cells without compromising ALP activity. The fluorescence microscopy assay was performed at a different time of the naphthol AS-MX flow cytometry assay, one week later.

5.3 Future perspectives

In terms of future perspectives related to this thesis, the essential remark to take from this work is how much is important to prepare the NPs in a sterile environment. In the last part of the experimental work this, PCLSOD and PCLALP NPs were prepared in a sterile environment and with sterile compounds, but it was not possible to repeat the delivery assays. In the future, these assays are essential to be performed again and with the same sterile set of PCLALP and PCLSOD NPs to obtain precise results and clear conclusions.

After performing these assays again, it will be possible to get answers to the questions: what is more effective, free SOD and free ALP, or ALP and SOD encapsulated into PCL NPs? And the reaction between the ALP substrate is occurring in the extracellular or intracellular domain?

It could also be interesting to see in which endocytosis compartment is occurring the enzyme's reactions, and verify endosomal escaping.

For the SOD approach, it can also be interesting to test the PCL capability of inducing oxidative stress in HeLa cells. Until our days, there are no references in the literature of these assays and it may be essential to see if PCL alone can induce some oxidative stress when entering in HeLa cells.

The results obtained for PCLALP were impressive, some of the NPs systems could successfully deliver ALP into HeLa cells, and in solution, PCL is capable of protecting the enzyme’s activity. But the contaminations may have lowered the enzyme activity, so it is important to repeat these assays with the sterile NPs.

As a general conclusion, it can be envisaged that if the PCL polymer is capable of formulating NPs encapsulating enzymes. This may have some impact in the enzyme delivery field, to overcome some barriers of enzyme replacement therapy.

REFERENCES

1. McClements, D. J. Encapsulation, protection, and delivery of bioactive proteins and peptides using nanoparticle and microparticle systems: A review. *Adv. Colloid Interface Sci.* (2018). DOI:10.1016/j.cis.2018.02.002

2. Heyman, M. B. & Care, P. Lactose Intolerance in Infants, Children, and Adolescents. *Am. Acad. Pediatr.* **118**, 1279–1286 (2006).

3. Hayes, D. G. Mechanism of Protein Extraction from the Solid State by Water-in-Oil Microemulsions. 584–591 (1997).

4. Foegeding, E. A. & Davis, J. P. Food Hydrocolloids Food protein functionality : A comprehensive approach. *Food Hydrocoll.* **25**, 1853–1864 (2011).

5. Lundquist, P. & Artursson, P. Oral absorption of peptides and nanoparticles across the human intestine: Opportunities, limitations, and studies in human tissues. *Adv. Drug Deliv. Rev.* (2016). DOI:10.1016/j.addr.2016.07.007

6. Wang, K. *et al.* Nanotopographical Modulation of Cell Function through Nuclear Deformation. *ACS Appl. Mater. Interfaces* **8**, 5082–5092 (2016).

7. Walther, R., Rautio, J. & Zelikin, A. N. Prodrugs in medicinal chemistry and enzyme prodrug therapies. *Advanced Drug Delivery Reviews* **118**, 65–77 (2017).

8. Baldo, B. A. Enzymes approved for human therapy: Indications, mechanisms, and adverse effects. *BioDrugs* **29**, 31–55 (2015).

9. Mendes, P. M. Cellular nanotechnology: Making biological interfaces smarter. *Chemical Society Reviews* **42**, 9207–9218 (2013).

10. Safari, A., Khiavi, M. A., Mousavi, R., Barar, J. & Rafi, M. A. Enzyme replacement therapies: What is the best option? *BioImpacts* **8**, 153–157 (2018).

11. Ryoo, H. D. & Bergmann, A. The role of apoptosis-induced proliferation for regeneration and cancer. *Cold Spring Harbor Perspectives in Biology* **4**, (2012).

12. Yuan, H., Li, N. & Lai, Y. Evaluation of in vitro models for screening alkaline phosphatase-mediated bioconversion of phosphate ester prodrugs. *Drug Metab. Dispos.* **37**, 1443–1447 (2009).

13. Jornada, D. H. *et al.* The prodrug approach: A successful tool for improving drug solubility. *Molecules* **21**, (2016).

14. Vellard, M. The enzyme as a drug: application of enzymes as pharmaceuticals. *Curr. Opin. Biotechnol.* **14**, 444–50 (2003).

15. Concolino, D., Deodato, F. & Parini, R. Enzyme replacement therapy : efficacy and limitations. *Ital. J. Pediatr.* **44**, (2018).

16. Zawilska, J. & Olejniczak. Prodrugs:A challenge for the drug development. *Pharmacol. Reports* **65**, 2–14 (2013).

17. Bafana, A., Dutt, S., Kumar, S. & Ahuja, P. S. Superoxide dismutase: An industrial perspective. *Critical Reviews in Biotechnology* **31**, 65–76 (2011).

18. Case, A. J. On the Origin of Superoxide Dismutase : An Evolutionary Perspective of Superoxide-Mediated Redox Signaling. *Antioxidants* **82**, (2017).

19. Enzymic, A. N. & Erythrocuprein, F. O. R. Superoxide Dismutase An enzymic function for erythrocuprein (hemocuprein). *J. Biol. Chem.* **244**, 6049–6055 (1969).

20. Lisboa Vendrell Marques Peralta, J. Phosphorylation by alkaline phosphatase: use of the enzyme in cascade reactions. (Instituto Superior Técnico, 2010).

21. Xiong, S., Mu, T., Wang, G. & Jiang, X. Mitochondria-mediated apoptosis in mammals. *Protein Cell* **5**, 737–749 (2014).

22. Rosenberg, S. H. Mammalian apoptosis in a parasitic worm. *Proc. Natl. Acad. Sci.* **108**, 6695–6696 (2011).

23. Murphy, M. P. How mitochondria produce reactive oxygen species. *Biochimie* **13**, 1–13 (2009).

24. Petrache, I. *et al.* Superoxide dismutase protect against apoptosis and alveolar enlargement induced by ceramide. *Am. J. Physiol. Cell. Mol. Physiol.* **295**, L44–L53 (2008).

25. Saccon, R. A., Bunton-stasyshyn, R. K. A., Fisher, E. M. C. & Fratta, P. Is SOD1 loss of function involved in amyotrophic lateral

sclerosis ? *Brain* 1–17 (2013). DOI:10.1093/brain/awt097

26. Conte-Daban, A. *et al.* A Metallo Pro-Drug to Target CuII in the Context of Alzheimer's Disease. *Chem. - A Eur. J.* **24**, 5095–5099 (2018).

27. Che, M., Wang, R., Li, X., Wang, H.-Y. & Zheng, X. F. S. Expanding roles of superoxide dismutases in cell regulation and cancer. *Drug Discov. Today* **21**, 143–149 (2016).

28. Kost, O. A. *et al.* Superoxide dismutase 1 enzyme for the treatment of eye inflammation. *Oxid. Med. Cell. Longev.* **2016**, (2016).

29. Singh, S. Nanomaterials Exhibiting Enzyme-Like Properties (Nanozymes): Current Advances and Future Perspectives. *Front. Chem.* **7**, 1–10 (2019).

30. Reddy, M. K., Wu, L. & Kou, W. Superoxide Dismutase-Loaded PLGA Nanoparticles Protect Cultured Human Neurons Under Oxidative Stress. *Appl Biochem Biotechnol* **151**, 565–577 (2008).

31. Sharma, U., Pal, D. & Prasad, R. Alkaline Phosphatase: An Overview. *Indian J. Clin. Biochem.* **29**, 269–278 (2014).

32. Coleman, J. E. Structure and mechanism of alkaline phosphatase. *Annu. Rev. Biophys. Biomol. Struct.* **21**, 441–83 (1992).

33. Siffert, B. R. S. The Role of Alkaline Phosphatase in Osteogenesis. *J. Exp. Med.* **93**, 415–426 (1950).

34. Golub, E. E. & Boesze-Battaglia, K. The role of alkaline phosphatase in mineralization. *Lippincott Williams and Wilkins* **18**, 444–448 (2007).

35. Sun, H. & Wang, Y. Novel Ser/Thr Protein Phosphatases in Cell Death Regulation. *Physiology* **27**, 43–52 (2012).

36. Kondratskyi, A., Kondratska, K., Skryma, R. & Prevarskaya, N. Ion channels in the regulation of apoptosis. *BBA - Biomembr.* 1–15 (2014). doi:10.1016/j.bbamem.2014.10.030

37. Farley, J. R. & Stilt-Coffing, B. Apoptosis May Determine the Release of Skeletal Alkaline Phosphatase Activity from Human Osteoblast-Line Cells. *Springer-Verlag New York* (2001). DOI:10.1007/s002230001181

38. Sharma, U., Pal, D., Singh, S. K., Kakkar, N. & Prasad, R. Reduced L/B/K alkaline phosphatase gene expression in renal cell carcinoma: Plausible role in tumorigenesis. *Biochimie* **104**, 27–35 (2014).

39. Chengfan Wu, Rui Zhang, Wei Du, Liang Cheng, G. L. Alkaline Phosphatase-Triggered Self-Assembly of Near-Infrared Nanoparticles for Enhanced Photoacoustic Imaging of Tumor. *Nano Lett.* 2–14 (2018). DOI:10.1021/acs.nanolett.8b03482

40. Sato, M. & Webster, T. J. Nanobiotechnology : implications for the future of nanotechnology in orthopedic applications. *Med. Devices* 105–114 (2004).

41. Liu, L., Hao, Y., Deng, D. & Xia, N. Nanomaterials-Based

Colorimetric Immunoassays. *Nanomaterials* **9**, 1–32 (2019).

42. Bolhassani, A., Javanzad, S., Saleh, T., Hashemi, M. & Aghasadeghi, M. R. Potent vectors for vaccine delivery targeting cancer and infectious diseases Polymeric nanoparticles. *Landes Biosci.* 321–332 (2014). doi:http://dx.doi.org/10.4161/hv.26796

43. Rana, V. & Sharma, R. *Chapter 5 - Recent Advances in Development of Nano Drug Delivery*. *Applications of Targeted Nano Drugs and Delivery Systems* (Elsevier Inc., 2019). DOI:10.1016/B978-0-12-814029-1.00005-3

44. Yadav, H. K. S., Almokdad, A. A., Sumia, I. M. & Debe, M. S. *Chapter 17 - Polymer-Based Nanomaterials for Drug-Delivery Carriers*. *Nanocarriers for Drug Delivery* (Elsevier Inc., 2019). DOI:10.1016/B978-0-12-814033-8.00017-5

45. Ravi, P. R., Vats, R., Dalal, V., Gadekar, N. & Aditya, N. Design, optimization and evaluation of poly- e -caprolactone (PCL) based polymeric nanoparticles for oral delivery of lopinavir. *Inf. Healthc.* **9045**, 1–10 (2013).

46. Shah, L. K. & Amiji, M. M. Intracellular Delivery of Saquinavir in Biodegradable Polymeric Nanoparticles for HIV / AIDS. *Pharm. Res.* **23**, 2638–2645 (2006).

47. Lemoine, D. *et al.* Stability study of nanoparticles of and poly (D, L-lactide-co-glycolide). *Biomaterials* **17**, 2191–2197 (1996).

48. Associate, A. *User Guide: Pierce BCA Protein Assay Kit (MAN0011430 Rev. A)*.

49. Sigma-Aldrich. *Intracellular Hydrogen Peroxide Assay Kit - Green Fluorescence*. (2014).

50. Halawa, A. A., Hamed, M. F., Balboula, A. Z. & Elmetwally, M. A. Lipopolysaccharide Prompts Oxidative Stress and Apoptosis in Rats' Testicular Tissue. *J. Vet. Healthc.* 20–31 (2013). DOI:10.14302/issn.2575-1212.jvhc-18-2013

51. Noworyta-Sokolowski, K., Górska, A. & Goembiowska, K. *LPS-induced oxidative stress and inflammatory reaction in the rat striatum*. *Pharmacological Reports* (2013).

52. Victor, V. M., Rocha, M. & De, M. Immune cells : free radicals and antioxidants in sepsis. *Int. Immunopharmacol.* **4**, 327–347 (2004).

53. Dean, R. L. *Kinetic Studies with Alkaline Phosphatase in the Presence and Absence of Inhibitors and Divalent Cations*. (2002).

54. Kindl, E. D., Koschnitzke, K. E., Blauwkamp, J. A., Mccann, S. M. & Veronica, R. Fluorescence of Naphthol AS-MX is Readily Detectable in Dioxane Mixtures. *Matters* 1–6 (2019). doi:10.19185/matters.201905000003

55. Research), M. S. B. (National I. of D. Histochemical Demonstration of Acid Phosphatases With Naphthol AS-Phosphates. *Oxford Journals* **21**, 523–539 (1958).

56. Caucho, C. I. C. & Barros, M. T. Polymeric nanoparticles: A study on the preparation variables and characterization methods. *Materials Science and Engineering C* **80**, 771–784 (2017).

57. Abdelwahed, W., Dagobert, G., Stainless, S. & Fessi, H. Freeze-drying of nanoparticles : formulation, process, and storage considerations ☆. *Elsevier* **58**, 1688–1713 (2006).

58. Coulter, B. *User ' s Manual-Delsa Nano Submicron Particle Size and Zeta Potential*. (2011).

59. Becton, D., and C. *Introduction to Flow Cytometry : A Learning Guide*. (2002).

60. Zhang, R., Ji, J. & Blaženovi, I. Investigation into Cellular Glycolysis for the Mechanism Study of Energy Metabolism Disorder Triggered by Lipopolysaccharide. *Toxins (Basel).* **10**, 1–13 (2018).

61. Pagani, R., Pen, J., Concepcio, M. & Porthole, M. T. Transitory oxidative stress in L929 fibroblasts cultured on poly (-caprolactone) films. *Elsevier* **26**, 5827–5834 (2005).

62. Singh, M., Sharma, H. & Singh, N. Hydrogen peroxide induces apoptosis in HeLa cells through the mitochondrial pathway. *Mithocodrion* **7**, 367–373 (2007).

APPENDIX

Appendix A - LPS calibration curve with a range of different LPS concentrations (µg/ml)

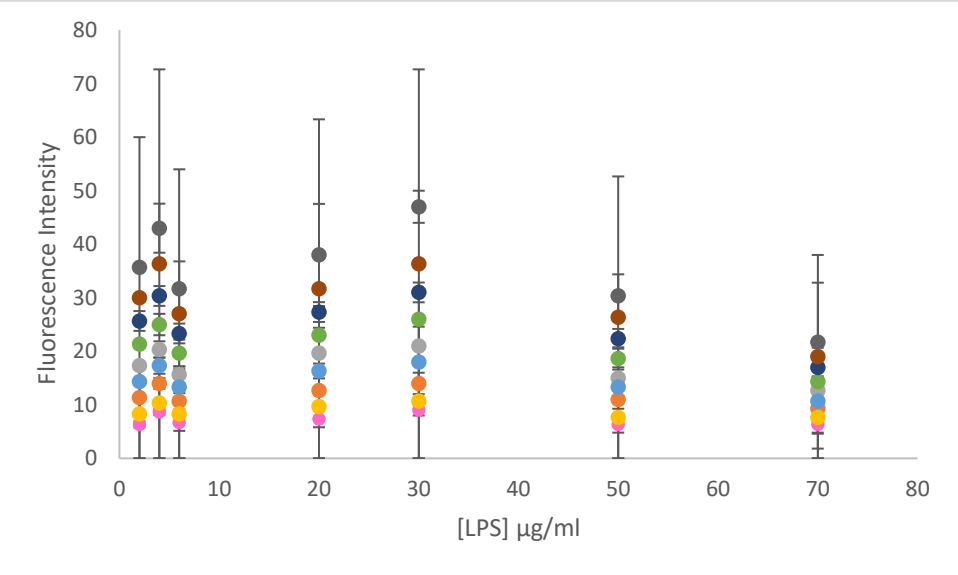

Figure A – LPS calibration curve, with different LPS concentrations: 0 µg/ml, 2 µg/ml, 4 µg/ml, 6 µg/ml, 20 µg/ml, 30 µg/ml, 50 µg/ml, and 70 µg/ml. Through different incubation times: Pink it is represented the 10 minutes of incubation time, Yellow it is represented the 20 minutes of incubation time, Orange it is represented the 20 minutes of incubation time, Blue it is represented the 40 minutes of incubation time, Clear grey it is represented the 50 minutes of incubation time, Green it is represented the 60 minutes of incubation time, Red it is represented the 80 minutes of incubation time, and Dark grey it is represented the 90 minutes of incubation time. The results were acquired in a microplate reader Bioteck synergy h1, and the assay was performed in triplicates.